treated within 4.5 h of onset, owing to the substantial risk of intracranial hemorrhage [6–8].

To overcome the limitations of conventional fibrinolytic therapy, the cavitational and non-cavitational effects of ultrasound (USD) have been studied and tested in conjunction with thrombolytic agents to facilitate thrombus disruption [9–16]. Treatment without the use of a thrombolytic agent, but with the combination of echo contrast microbubbles and USD, has been found to be effective *in vitro* and *in vivo*. This has been theorized to be attributable to a lower cavitational threshold and enhanced microstreaming phenomena when microbubbles in conjunction with USD are used [17–23]. *In vivo*, transcutaneous USD in combination with microbubbles has been reported to recanalize thrombotically occluded iliofemoral, coronary and ascending pharyngeal arteries [18,20–22], reduce infarction size [23] and improve microvascular recovery [20] in animal models, without significant side effects. Clinical trials using transcutaneous USD with microbubbles in the setting of ischemic stroke have not been conducted; instead, a combination of USD, microbubbles and thrombolytic agents has been examined. This combination strategy improves recanalization rates and preserves brain function as compared with USD and thrombolytic agents without microbubbles [24–27]. However, an increased number of intracranial hemorrhages has also been reported [27].

In order to non-invasively detect thrombus location, we manufactured thrombus-targeted liposomal bubbles (bubble liposomes [BLs]), which we also expected to enhance ultrasonic clot disruption. These BLs may avoid the need for invasive angiography to identify the thrombotically occluded site prior to the application of therapeutic USD in *in vivo* studies [18,20–22]. The BL was composed of perfluorocarbon gas-containing nanosized liposomes with Arg-Gly-Asp (RGD) sequence peptides on their surface lipid layer, which attach glycoprotein IIb–IIIa complex on activated platelets and enhance the visualization of fresh thrombus by conventional diagnostic ultrasound examination [28]. We hypothesized that these thrombus-targeted BLs could also enhance disruption with the use of therapeutic external USD, and could be used to develop a fully non-invasive diagnostic and therapeutic system for the treatment of thrombotic vessel occlusion. The aim of this study was to examine the enhancing effect of the newly developed thrombus-targeted liposomal bubbles on ultrasonic disruption of the thrombus *in vitro* and *in vivo*.

Materials and methods

Preparation of thrombus-targeted BLs

Liposome-based perfluorocarbon-containing BLs were composed of 126 mg of 1,2-disteoyl-*sn*-glycero-phosphocholine (Avanti, Alabaster, AL, USA), 51 mg of 1,2-distearoyl-*sn*-glycero-3-phosphatidylethanolamine-*m*-polyethylene glycol 2000 with maleimide (Avanti), 30 mg of cholesterol (Sigma-Aldrich, Tokyo, Japan), CGGGRGDF peptide (Operon Biotechnologies, Tokyo, Japan), and perfluoropropane gas (Takachiho, Tokyo, Japan). We previously reported the manufacture of these liposome-based perfluorocarbon-containing BLs [28]. In brief, a mixture of all reagents except for CGGGRGDF peptide and perfluoropropane gas was dissolved in 2.0 mL of chloroform, and mixed with the same amount of di-isopropyl ether and normal saline. The mixture was sonicated, with a probe-type 19.5-kHz ultrasound device at 550 W (XL-2020 Sonicator; Misonix, Farmingdale, NY, USA), and then evaporated at 65 °C with a rotary evaporating system (Tokyo Rika, Tokyo, Japan). After the chemical solvent had been completely removed, the size of liposomes was adjusted to < 0.2 μm with extruding equipment and a membrane filter (Northern Lipids, Vancouver, Canada) with sizing filters. To the liposome liquid, 1 mg of linear octapeptide with the sequence CGGGRGDF (Operon Biotechnologies) was added, and allowed to conjugate to the maleimide on the liposomal surface via thio–ether covalent coupling at room temperature for 2 h. Gel filtration was then used to remove unreacted peptide fragments. The lipid concentration was measured with the Wako Phospholipid C test (Wako Pure Chemical Industries, Osaka, Japan) and the RGD-liposomes were diluted to a final concentration of 20 mg mL^{-1}. The RGD-liposomes were sealed in a 5-mL vial, and air was exchanged with perfluoropropane gas (Takachiho); this was followed by 20-kHz USD treatment with a bath-type sonicating system (Model 3510; Branson, Emerson, CT, USA) for 5 min to generate the RGD-BLs [28]. Sterile filtration (0.45 μm) was then performed to remove the expanded and oversized BLs. Non-targeted BLs were prepared with the same methods but without the addition of RGD peptide. The amount of perfluoropropane gas trapped in the BLs was estimated to be ~ 10 μL mg^{-1} lipid, and the diameter of each BL was 180 ± 44 nm as measured by dynamic laser light-scattering measurements with an ELS-800 particle analyzer (Otsuka Photonics, Tokyo, Japan).

Therapeutic USD system

For both *in vitro* and *in vivo* studies, two different USD systems (low intensity or high intensity) were used. For the low-intensity USD study, the Timi3 system was used (Timi3 Systems, Santa Clara, CA, USA). This device consisted of a low-frequency USD generator (maximum intensity, 1.4 W cm^{-2}) and a transducer that delivered 27 kHz of USD at a pulse rate of 25 Hz (acoustic pressure, 0.145 MPa; mechanical index, 1.4). For the high-intensity study, the therapeutic USD system was composed of a sine wave pulse generator (MG-422A; Anritsu, Tokyo, Japan), a radiofrequency power amplifier

(2100L; ENI, Rochester, NY, USA), and a prototype piezoelectric transducer (Fuji Ceramics, Shizuoka, Japan). The transducer consisted of 10 PZT disks (thickness, 4 mm) tightly bonded together. It was operated in a continuous-wave mode at a frequency of 27 kHz (acoustic pressure, 0.346 MPa; mechanical index, 3.2) and an intensity of 4.0 W cm^{-2} as measured by the calorimetric method [29].

Protocol for in vitro *study on human thrombi*

The following *in vitro* investigation conforms with the principles outlined in the Declaration of Helsinki, and the protocol was approved by the Ethical Committee of the National Defense Medical College. In total, 60 thrombi were used in this *in vitro* study. For the preparation of each thrombus, 9 mL of whole blood was collected in a test tube from a healthy volunteer, placed on a seesaw-type shaker, and allowed to coagulate at room temperature while being shaken and rotated at a speed of 60 r.p.m. for 1 h. Targeted BLs or non-targeted BLs (100 μL, 20 mg mL^{-1} lipid concentration, ~ 1.1% v/v) were added to the test tube 10 min after the initiation of coagulation. The formed thrombus was washed with normal saline, cut into small pieces, weighed on an electronic balance, and placed in a plastic test tube containing 2 mL of human plasma. Before the therapeutic USD exposure, attachment of the BLs on the clot was confirmed by conventional USD imaging, as well as by scanning electron microscopy [28]. The test tube was placed at 1 cm from the therapeutic USD transducer in a bath filled with degassed water. Thirty thrombi were exposed to low-intensity USD: 10 without BLs as controls, 10 with non-targeted BLs, and 10 with targeted BLs. Similarly, 30 thrombi were exposed to high-intensity USD: 10 without BLs as controls, 10 with non-targeted BLs, and 10 with targeted BLs. The water temperature was maintained at 37 °C. Each thrombus was exposed to low-intensity USD (27 kHz, 1.4 W cm^{-2}) or high-intensity USD (27 kHz, 4.0 W cm^{-2}) for 5 min. After USD exposure, the clot was weighed again. The thrombus weight reduction rate ([pre-treatment weight – post-treatment weight]/pre-treatment weight × 100 [%]) was calculated as an index of the thrombolytic effect.

In vivo *study protocol in an acute thrombotic occlusion model of a rabbit iliofemoral artery*

The animal protocol was approved by the Animal Care and Use Committee of the National Defense Medical College, and conformed with the Guide for the Care and Use of Laboratory Animals published by the US National Institutes of Health (NIH Publication, 8th Edition, 2011).

A total of 54 New Zealand white rabbits (~ 2.4 kg) were used: 24 for the low-intensity USD study, 20 for the high-intensity USD study, and 10 for the fibrinolysis study. Each rabbit was anesthetized with 50 mg of ketamine and 20 mg of xylazine injected intramuscularly, and anesthesia was maintained with pentobarbital (15 mg kg^{-1}) delivered via a marginal ear vein. The adequacy of anesthesia was monitored by the loss of the ear pinch reflex. Anesthetized rabbits were placed on a warming plate to maintain the body temperature at 37 °C. Aseptic techniques were used for all surgical procedures. A 5Fr sheath was inserted into the right carotid artery, a balloon catheter was advanced to the right iliofemoral artery, and the intima was injured by balloon inflation and scratching. The balloon catheter was then pulled back, a 0.014-inch guide wire was positioned at the injured site, and electrical stimulation (3-V battery) was applied between the guide wire and skin electrode [18,21,28,30]. Thirty minutes later, the right iliofemoral artery was thrombotically occluded, and the arterial occlusion was confirmed by angiography. The thrombus was also imaged with a 9-MHz linear transducer and a conventional USD machine 1 min after BL injection (UF-750XT; Fukuda Denshi, Tokyo, Japan) (frame rate, 24–30/s; mechanical index, 0.3) (Fig. 1).

To determine the thrombolytic effect of targeted BLs and USD, we applied the low-intensity or high-intensity USD transcutaneously over the site of the rabbit iliofemoral arterial thrombus in combination with an intravenous injection of non-targeted BLs or targeted BLs. A total of 44 New Zealand white rabbits with iliofemoral

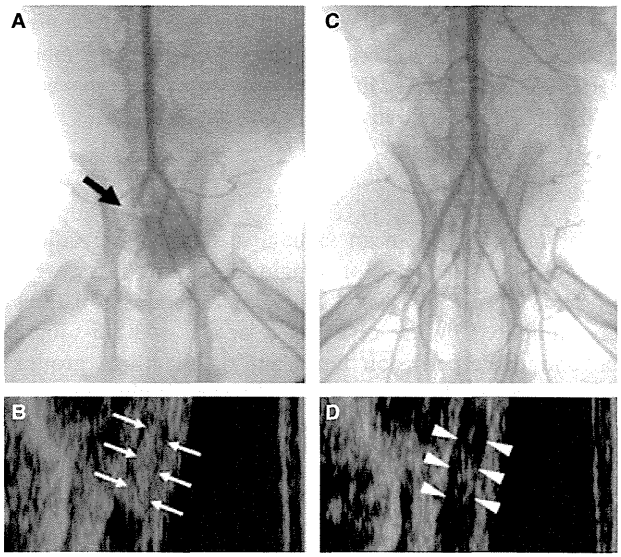

Fig. 1 . (A) Angiographic image of thrombotically occluded rabbit iliac artery (black arrow) after balloon inflation and electrical (3-V battery) stimulation. (B) In sonographic images, the targeted bubble liposomes (BLs) accumulated on the thrombus (white arrows). (C, D) After combination therapy with low-frequency ultrasound (USD) and thrombus-targeted BLs, TIMI grade 3 flow was achieved (C), and the high echogenic area within the iliac artery almost disappeared (white arrowheads) (D).

arterial occlusions were divided into two groups: 24 for low-intensity USD, and 20 for high-intensity USD. In both groups, non-targeted BLs were intravenously administered in half (12 or 10, respectively) of the rabbits, and targeted BLs were used in the other half (12 or 10, respectively) of the rabbits.

Before the USD exposure, 200 IU kg^{-1} heparin was injected intravenously. Angiography was performed every 15 min for a total of 90 min, and the TIMI blood flow grade was assessed [18,31]. Non-targeted or targeted BLs (1 mL, ~ 1.1% v/v) were intravenously injected every 15 min after the angiography. Subsequently, transcutaneous USD was applied externally over the site of the thrombus for 12 min. In the targeted BL and USD group, thrombus location was also confirmed with a diagnostic USD machine (UF-750XT; Fukuda Denshi) and with angiography (Fig. 1). BL injection and subsequent USD exposure were repeated four times for a total of 60 min. The vessel was observed for acute thrombotic reocclusion for the next 30 min. The recanalization (TIMI grade 3 flow) rate was calculated, and the reperfusion time was measured only in cases in which reperfusion was achieved. All of the angiographic assessments represented the consensus of two expert cardiologists (T.N. and B.T.) blinded to group allocation.

In 10 New Zealand white rabbits with iliofemoral arterial occlusions, 27 500 IU kg^{-1} recombinant tissue plasminogen activator (rt-PA) (Monteplase, Eizai, Tokyo, Japan) was intravenously administered within a period of 1 min immediately after intravenous injection of 200 IU kg^{-1} heparin. Angiography was repeated every 15 min for a total of 90 min, and the TIMI blood flow grade was assessed [18,31]. At the end of the experiment, all rabbits were killed with an overdose of pentobarbital (75 mg kg^{-1}) injected via a marginal ear vein.

Statistical analysis

Results are given as mean value ± 1 standard deviation. In the *in vitro* study, clot weight reduction rates were compared by use of ANOVA. *In vivo*, the reperfusion rates were compared by use of a 2 × 2 or a 2 × 3 chi-square test, and the reperfusion times among the three groups were compared by use of the Kruskal–Wallis test. A *P*-value of < 0.05 was considered to be statistically significant.

Results

In vitro *study*

The clot weight reduction rate achieved with low-intensity USD with targeted BLs was significantly higher than that with the non-targeted BLs and in the controls without BLs (25% ± 11% vs. 14% ± 9% and 9% ± 3%, respectively; $P < 0.01$). Non-targeted BLs gave no significant enhancement of clot weight reduction (Fig. 2). Similarly, the clot weight reduction rate achieved with high-intensity USD in combination with targeted BLs was significantly higher than that with non-targeted BLs and in the controls (65% ± 21% vs. 21% ± 9% and 21% ± 14%, respectively; $P < 0.01$). No significant enhancement of clot weight reduction was observed when non-targeted-BLs were used.

On comparison of the effects of low-intensity USD and high-intensity USD, the clot weight reduction rate was significantly higher in the high-intensity USD group than in the low-intensity USD group when USD was applied without BLs (21% ± 9% vs. 9% ± 3%) and with targeted BLs (65% ± 21% vs. 25% ± 11%).

In both groups, echo signal enhancement of all thrombi by targeted BLs declined to control and non-targeted BL levels after USD exposure.

In vivo *low-intensity USD study*

Rabbit iliofemoral arterial thrombus was clearly recognized with a conventional USD system with the targeted BLs, and also confirmed by angiography (Fig. 1). The Doppler signal enhancement of the iliofemoral arterial flow by both targeted and non-targeted BLs was observed even at 12 min after therapeutic USD irradiation. TIMI grade 3 flow was achieved in eight of 12 rabbits (67%) with targeted BL and USD exposure; however, TIMI grade 3 flow was achieved in only one of 12 rabbits (8%) in the non-targeted BL and USD group (Table 1; Fig. 3). These differences were statistically significant (targeted BLs, 67%; non-targeted BLs, 8%; $P = 0.003$). The time to reperfusion was ~ 40 min in the group with targeted

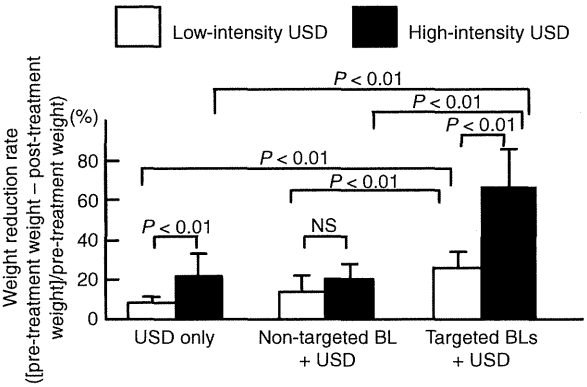

Fig. 2. The *in vitro* thrombus weight reduction rate ([pre-treatment weight – post-treatment weight]/pre-treatment weight × 100 [%]) obtained with low-frequency ultrasound (USD): high-intensity USD exposure for 5 min with the targeted bubble liposomes (BLs), with the non-targeted BLs, or without BLs ($P < 0.01$, $n = 10$, ANOVA); low-intensity USD exposure for 10 min with the targeted BLs, with the non-targeted BLs, or without BLs ($P < 0.01$, $n = 10$, ANOVA). The clot weight reduction rate increased with therapeutic USD with targeted BLs in each intensity study. NS, not significant.

BL and USD exposure (Table 1). There were three cases of blood flow reduction (TIMI grade 3 to 2) during the observation period in the targeted BL group (Fig. 3).

In vivo *high-intensity USD study and fibrinolysis study*

After exposure to low-frequency high-intensity transcutaneous USD, TIMI grade 3 flow was achieved in nine of 10 rabbits (90%) with targeted BLs. On the other hand, recanalization was achived in only two of 10 rabbits (20%) with USD and non-targeted BLs, and four of 10 arteries (40%) were recanalized with rt-PA monotherapy (Table 2; Fig. 4). These differences were statistically significant (targeted BLs, 90%; non-targeted BLs, 20%; rt-PA, 40%; $P = 0.004$). Moreover, the average reperfusion time for rabbits to achieve TIMI grade 3 flow was significantly shorter for those cases with high-intensity USD thrombolysis with targeted BLs than for those with high-intensity USD with non-targeted BLs or for those with ordinary thrombolysis with rt-PA (targeted BLs, 16.7 ± 5.0 min; non-targeted BLs, 60.0 ± 0 min; rt-PA, 41.3 ± 14.4 min; $P = 0.007$; $n = 10$) (Table 2). There were no cases of acute reocclusion, and all recanalized arteries maintained TIMI grade 3 flow, whereas two cases of acute reocclusion occurred during the procedure and the observation period in the non-targeted BL group (Fig. 4).

Table 1 Frequency of TIMI grade 3 flow (A) and time to each TIMI grade 3 flow (B) achieved with a combination of transcutaneous low-intensity ultrasound (USD) and targeted bubble liposomes (BLs) or non-targeted BLs

	Targeted BLs + USD	Non-targeted BLs + USD	*P*-value
(A)			
Frequency, no. (%)	8/12 (67)	1/12 (8)	0.003
(B)			
Mean time (min)	43.1 ± 20.3	60.0 ± 0	NA

NA, not applicable.

Discussion

This study demonstrated significant enhancement of ultrasonic thrombus disruption by the thrombus-targeted BLs and external low-frequency USD system *in vitro* and *in vivo*, and the possibility of a completely non-invasive treatment that combines the identification of thrombus position with rapid clot disruption. This study validates the use of the low-frequency USD system with targeted BLs for rapid, effective and comprehensive thrombolytic treatment. The combination of USD and targeted BLs played a primary role in this study in both the diagnosis and treatment of thrombotic vascular occlusions.

In many of the previous studies dealing with *in vivo* USD clot disruption and using microbubbles to reinforce the USD energy, invasive angiography was used to identify the precise location of the thrombus, and to guide the manipulation of the therapeutic USD probe [9,10,18,21]. Otherwise, transcranial Doppler was used to monitor deteriorated blood flow, or a large transducer was used to cover the area of vessel occlusion [25–27,32]. Recently, we developed thrombus-targeted liposomal bubbles for USD imaging of fresh thrombus. This *in vitro* and *in vivo*

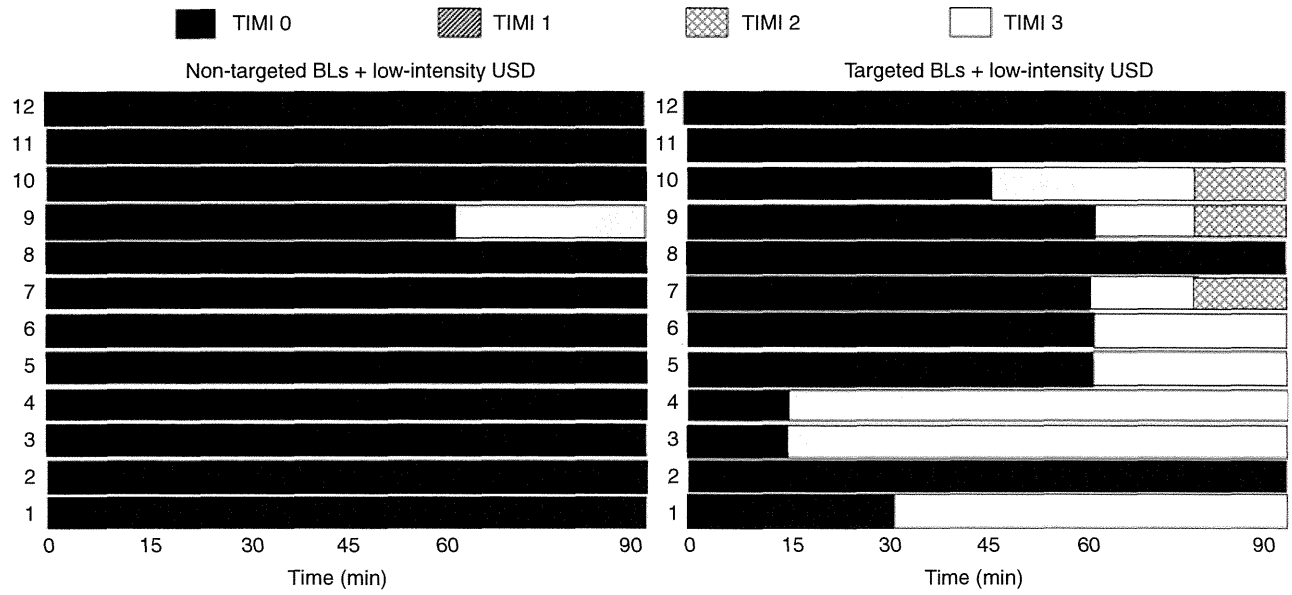

Fig. 3. Schematic presentation showing TIMI flow grades of the arteries treated with low-intensity ultrasound (USD) with non-targeted bubble liposomes (BLs) and targeted BLs. TIMI grade 3 flow was achieved in 67% of arteries with targeted BLs and in only 8% of arteries with non-targeted BLs ($P = 0.003$, 2 × 2 chi-square test).

study showed that the USD image of thrombus could be identified at a glance with a conventional diagnostic USD machine with the targeted BLs, as also found in our previous study [28]. This enhanced thrombus imaging facilitated successful USD thrombolysis without invasive angiography.

The targeted BLs significantly enhanced ultrasonic clot disruption *in vitro* and *in vivo* when used with both low-intensity and high-intensity USD. In particular, with high-intensity USD exposure with targeted BLs *in vivo*, arterial recanalization was achieved in 90% of acute thrombotically occluded rabbit iliofemoral arteries within 20 min from the beginning of the diagnostic procedure. This speed of treatment potentially surpasses that of the PCI procedures, which, on average, require at least 90 min to achieve reperfusion from arrival at the hospital [3]. This rapid and non-invasive therapy shows promise in acute cardiovascular medicine, as diagnostic and therapeutic USD equipment is compact in size, inexpensive, and does not require dedicated laboratory space and specialized PCI staff.

These results were equivalent to those of the sonothrombolysis study by Culp *et al.*, in which a combination of 2-MHz USD and eptifibatide-tagged microbubbles opened acute intracranial thrombotic occlusions in six of eight pigs without the use of a thrombolytic agent [22]. Recently, Alonso *et al.* reported that diagnostic 2-MHz USD in combination with abciximab immunobubbles induced thrombolysis (increased plasma D-dimer levels) without lytic agents in rats [33]. However, the arterial recanalization was not assessed, as a partial thrombotic occlusion model of the rat carotid artery was used. Xie *et al.* also reported that diagnostic USD (1.5 MHz) treatment with platelet-targeted microbubbles in combination with half-dose recombinant prourokinase gave a 53% coronary arterial recanalization rate at 30 min in pigs [20]. These studies demonstrate that clinically used diagnostic USD frequencies can be applied to thrombus dissolution with thrombus-targeted microbubbles. However, their thrombolytic effect was relatively limited, except for the intracranial model [22], presumably because the cavitational energy generated by high-frequency USD (MHz) and microbubbles was relatively low in the absence of a closed space such as a skull, where USD energy could be enhanced by standing wave formation [34]. To overcome this limitation, we used low-frequency (kHz) USD as a therapeutic device to achieve a higher recanalization rate.

Table 2 Frequency of TIMI grade 3 flow (A) and time to each TIMI grade 3 flow (B) achieved with a combination of transcutaneous high-intensity ultrasound (USD) and targeted bubble liposomes (BLs) or non-targeted BLs, or recombinant tissue-type plasminogen activator (rt-PA) alone

	Targeted BLs + USD	Non-targeted BLs + USD	rt-PA	*P*-value
(A) Frequency, no. (%)	9/10 (90)	2/10 (20)	4/10 (40)	0.004
(B) Mean time (min)	16.7 ± 5.0	60.0 ± 0	41.3 ± 14.4	0.007

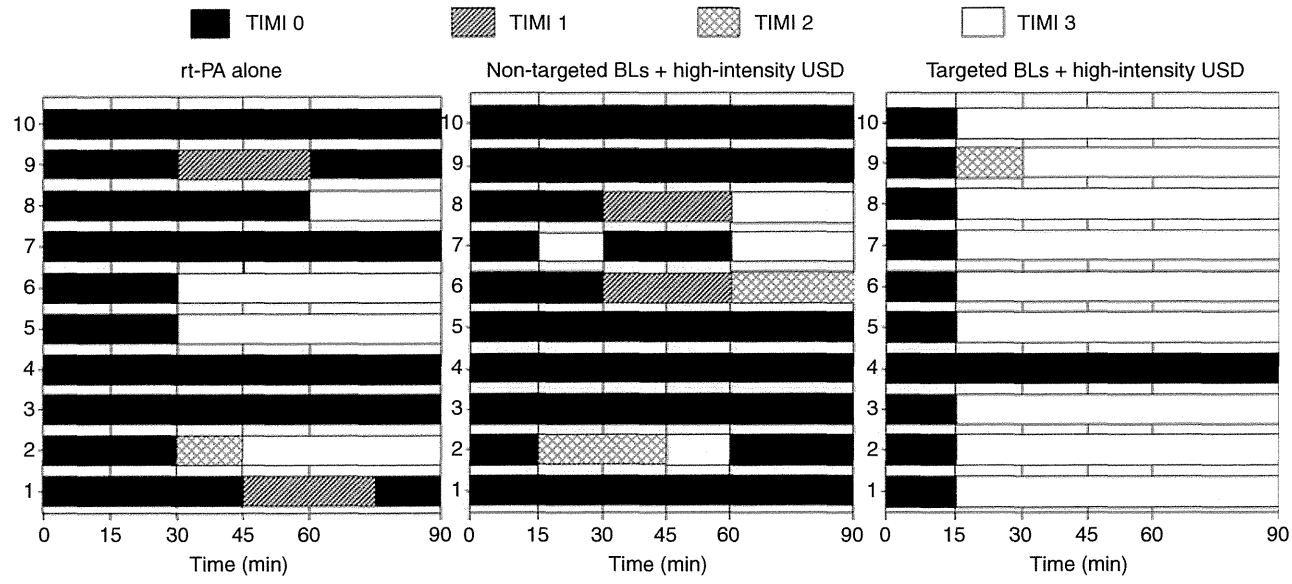

Fig. 4. Schematic presentation showing TIMI flow grades of the arteries treated with recombinant tissue-type plasminogen activator (rt-PA) alone, with high-intensity ultrasound (USD) with non-targeted bubble liposomes (BLs), and with high-intensity USD with targeted BLs. TIMI grade 3 flow was achieved in 90% of arteries treated with USD with targeted BLs, in only 20% of arteries treated with USD with non-targeted BLs, and in 40% of arteries treated with rt-PA monotherapy ($P = 0.02$, 2 × 3 chi-square test).

Low-frequency USD is advantageous, because it penetrates deeper into tissue and has less thermal effect than high-frequency USD [35]. Low-frequency USD has been reported to recanalize canine iliofemoral and coronary arteries without tissue damage [9,10,21,36], and has been safely applied in combination with thrombolytic agent in humans with STEMI [13], with a USD intensity as low as that used in our low-intensity USD study. However, there are still safety concerns regarding the application of high-intensity, low-frequency USD with microbubbles, and these should be clarified in a future study.

Nano-sized BLs could have some potential disadvantages. It is assumed that BLs release less energy than larger microbubbles when they collapse. In fact, the non-targeted BLs showed negligible enhancement of USD clot disruption *in vitro*. Moreover, only 8–20% cases of thrombosed rabbit iliofemoral arteries recanalized *in vivo* with non-targeted BLs. Theoretically, each BL itself is too small to reflect USD waves with the frequency used in this study. However, we previously demonstrated that the targeted BLs are highly concentrated around and within the thrombus, by using scanning electron microscopy, and that they markedly enhance ultrasonic thrombus imaging [28]. Consequently, as shown in this *in vitro* and *in vivo* study, we found marked enhancement of the thrombolytic effect by attaching the thrombus-targeting ligands on the same BL structure. The small size of the BLs, with a mean diameter of 180 nm, could also have some advantageous effects. A BL size of <1 μm ensures both a long *in vivo* circulation time and deep penetration into thrombi. The longer the circulation time, the more opportunity the targeted BL has to attach to the activated thrombus. Deep penetration into thrombi through the fibrin network allows for greater accumulation of targeted BLs within thrombi. These two features of small BLs were favorable, when USD energy was applied, for disruption and reduction of the culprit thrombus.

Liposomes are usually considered to be non-toxic, unless they are administered at very high doses [37]. Polyethylene glycol is also considered to be non-toxic, and is excreted unmetabolized in the urine [38]. The RGD peptide is an octapeptide, and is considered to be non-toxic and non-immunogenic [39,40]. Perfluoropropane is an inert gas, used as a constituent of commercially available echo contrast agents such as Optison and Definity [41], and is exhaled from the lungs [42]. Therefore, this echo contrast agent is generally considered to be non-toxic, although safety in humans remains to be demonstrated.

In a clinical setting, lower-intensity USD has some advantages over high-intensity USD in terms of safety. However, low-intensity USD exposure with targeted BLs achieved only a modest thrombolytic effect in this study. When low-intensity USD is used, an alternative approach is necessary to enhance the resonance phenomenon caused by the interaction between USD and the BLs. As the RGD peptide is not an ideal targeting ligand, because of its broad cross-reactivity with a number of integrins, one possible option is to achieve a higher concentration of the BLs on the thrombus by using a more effective targeting ligand. The other option is to use larger BLs, which generate a higher amount of cavitational energy during collapse. However, the BLs should be small enough to penetrate into the thrombus. Therefore, the most effective size of BLs remains to be determined. Another option is to combine targeted BL-enhanced USD thrombolysis with conventional fibrinolytic therapy. The dose of the fibrinolytic agent, such as tissue-type plasminogen activator, could be reduced with this strategy. Further study is needed to elucidate this issue.

The targeted BLs enhance imaging of the culprit thrombus and enable manipulation of the therapeutic USD probe, targeting and directing it towards the culprit thrombus. Furthermore, the combination treatment with targeted BLs and high-intensity, low-frequency USD achieved a 90% recanalization rate, which is markedly higher than that with rt-PA monotherapy. This method has the potential to be a reperfusion strategy that could be more rapid than any other method, including PCI. The absence of acute reocclusion with this therapeutic approach might be attributable to minimal mural thrombus being left in the culprit lesion. Further study is needed to identify the most suitable targeting ligand and BL size for generating the maximum thrombus disruption and achieving the most effective thrombolysis with low-intensity USD.

Limitations

There are some technical limitations regarding thrombus formation in both the *in vitro* study and the *in vivo* study. We prepared all *in vitro* clots from the blood of a single individual, to examine the effects of USD and targeted BLs on clots with homogeneous lytic activities. However, this could simultaneously be a limitation of this study, because individual lytic response can differ as a function of the different levels of inhibitory enzymes and/or varying concentrations of plasminogen. Moreover, *in vivo* hyperacute thrombi could be more fragile than those in clinical culprit lesions.

Reocclusion of the culprit artery was not observed after successful recanalization with low-frequency USD and targeted BLs. However, the observation period after recanalization in this study might not be long enough to exclude the possibility of reocclusion, which may occur later. There are some safety limitations. It is known from the simulation study of intracranial sonothrombolysis [34] that USD sometimes causes standing wave formation and unnecessary acoustic cavitation, especially in brain tissue, even outside the targeted clot. Regarding the coronary and peripheral arteries, low-frequency, high-intensity USD energy can be delivered transcutaneously for clot disruption without concomitant tissue damage in animal models,

especially when coupled with the use of a cooling system to prevent thermal injury [9,10,21,36]. However, low-frequency USD could cause unexpected non-linear cavitational effects, and its safety has to be clarified in combination with microbubbles before clinical application.

Conclusions

Perfluorocarbon gas-containing liposomal nanobubbles with activated thrombus-targeting RGD peptides developed for USD thrombus imaging are novel echo contrast agents that can markedly enhance USD thrombolysis both *in vitro* and *in vivo*. The combination of USD and thrombus-targeted BLs could be used as an effective and completely non-invasive recanalization therapy that does not require angiography to detect acute thrombotic vessel occlusion or therapeutic thrombus dissolution.

Addendum

K. Hagisawa, T. Nishioka, and R. J. Siegel: conception and design; K. Hagisawa, T. Nishioka, R. Suzuki, B. Takase, K. Iida, and H. Luo: acquisition of data; K. Hagisawa, T. Nishioka, and A. Kurita: analysis and interpretation of data; K. Hagisawa, T. Nishioka, and R. J. Siegel: drafting of the manuscript; K. Maruyama, M. Ishihara, N. Yoshimoto, and Y. Nishida: supervision.

Financial support

This study was supported in part by a Grant-in-Aid for Scientific Research (B) (16300176) from the Japan Society for the Promotion of Science, and a Japan Heart Foundation Research Grant.

Disclosure of Conflict of Interests

The authors state that they have no conflict of interest.

References

1 Mizuno K, Miyamoto A, Satomura K, Kurita A, Arai T, Sakurada M, Yanagida S, Nakamura H. Angioscopic coronary macromorphology in patients with acute coronary disorders. *Lancet* 1991; **337**: 809–12.

2 Fuster V, Fayad ZA, Badimon JJ. Acute coronary syndromes: biology. *Lancet*. 1999; **353**: SII5–9.

3 Antman EM, Anbe DT, Armstrong PW, Bates ER, Green LA, Hand M, Hochman JS, Krumholz HM, Kushner FG, Lamas GA, Mullany CJ, Ornato JP, Pearle DL, Sloan MA, Smith SC Jr, Alpert JS, Anderson JL, Faxon DP, Fuster V, Gibbons RJ, *et al.* ACC/AHA guidelines for the management of patients with ST-elevation myocardial infarction – executive summary: a report of the American College of Cardiology/American Heart Association Task Force on Practice Guidelines (Writing Committee to Revise the 1999 Guidelines for the Management of Patients With Acute Myocardial Infarction). *Circulation* 2004; **110**: 588–636.

4 Stone GW, Grines CL, Rothbaum D, Browne KF, O'Keefe J, Overlie PA, Donohue BC, Chelliah N, Vlietstra R, Catlin T, O'Neill WW. Analysis of the relative costs and effectiveness of primary angioplasty versus tissue-type plasminogen activator: the Primary Angioplasty in Myocardial Infarction (PAMI) trial. The PAMI Trial Investigators. *J Am Coll Cardiol* 1997; **29**: 901–7.

5 Schomig A, Kastrati A, Dirschinger J, Mehilli J, Schricke U, Pache J, Martinoff S, Neumann FJ, Schwaiger M. Coronary stenting plus platelet glycoprotein IIb/IIIa blockade compared with tissue plasminogen activator in acute myocardial infarction. Stent versus Thrombolysis for Occluded Coronary Arteries in Patients with Acute Myocardial Infarction Study Investigators. *N Engl J Med* 2000; **343**: 385–91.

6 Sandercock P, Wardlaw JM, Lindley RI, Dennis M, Cohen G, Murray G, Innes K, Venables G, Czlonkowska A, Kobayashi A, Ricci S, Murray V, Berge E, Slot KB, Hankey GJ, Correia M, Peeters A, Matz K, Lyrer P, Gubitz G, *et al.* The benefits and harms of intravenous thrombolysis with recombinant tissue plasminogen activator within 6 h of acute ischaemic stroke (the Third International Stroke Trial [IST-3]): a randomised controlled trial [published correction appears in *Lancet*. 2012; 380: 730]. *Lancet* 2012; **379**: 2352–63.

7 Jauch EC, Saver JL, Adams HP Jr, Bruno A, Connors JJ, Demaerschalk BM, Khatri P, McMullan PW Jr, Qureshi AI, Rosenfield K, Scott PA, Summers DR, Wang DZ, Wintermark M, Yonas H; American Heart Association Stroke Council; Council on Cardiovascular Nursing; Council on Peripheral Vascular Disease; Council on Clinical Cardiology. Guidelines for the early management of patients with acute ischemic stroke: a guideline for healthcare professionals from the American Heart Association/American Stroke Association. *Stroke* 2013; **44**: 870–947.

8 Wahlgren N, Ahmed N, Dávalos A, Hacke W, Millán M, Muir K, Roine RO, Toni D, Lees KR; SITS investigators. Thrombolysis with alteplase 3–4.5 h after acute ischaemic stroke (SITS-ISTR): an observational study. *Lancet* 2008; **372**: 1303–9.

9 Luo H, Birnbaum Y, Fishbein MC, Peterson TM, Nagai T, Nishioka T, Siegel RJ. Enhancement of thrombolysis in vivo without skin and soft tissue damage by transcutaneous ultrasound. *Thromb Res* 1998; **89**: 171–7.

10 Siegel RJ, Atar S, Fishbein MC, Brasch AV, Peterson TM, Nagai T, Pal D, Nishioka T, Chae JS, Birnbaum Y, Zanelli C, Luo H. Noninvasive, transthoracic, low-frequency ultrasound augments thrombolysis in a canine model of acute myocardial infarction. *Circulation* 2000; **101**: 2026–9.

11 Suchkova V, Carstensen EL, Francis CW. Ultrasound enhancement of fibrinolysis at frequencies of 27 to 100 kHz. *Ultrasound Med Biol* 2002; **28**: 377–82.

12 Laing ST, Moody M, Smulevitz B, Kim H, Kee P, Huang S, Holland CK, McPherson DD. Ultrasound-enhanced thrombolytic effect of tissue plasminogen activator-loaded echogenic liposomes in an in vivo rabbit aorta thrombus model – brief report. *Arterioscler Thromb Vasc Biol* 2011; **31**: 1357–9.

13 Hudson M, Greenbaum A, Brenton L, Gibson CM, Siegel RJ, Reeves LR, Sala MF, McKendall G, Bluguermann J, Echt D, Ohman EM, Weaver WD. Adjunctive transcutaneous ultrasound with thrombolysis: results of the PLUS (Perfusion by Thrombo-Lytic and UltraSound) trial. *JACC Cardiovasc Interv* 2010; **3**: 352–9.

14 Nedelmann M, Eicke BM, Lierke EG, Heimann A, Kempski O, Hopf HC. Low-frequency ultrasound induces nonenzymatic thrombolysis in vitro. *J Ultrasound Med* 2002; **21**: 649–56.

15 Alexandrov AV, Molina CA, Grotta JC, Garami Z, Ford SR, Alvarez-Sabin J, Montaner J, Saqqur M, Demchuk AM, Moyé LA, Hill MD, Wojner AW; CLOTBUST Investigators. Ultrasound enhanced systemic thrombolysis for acute ischemic stroke. *N Engl J Med* 2004; **351**: 2170–8.

16 Tsivgoulis G, Eggers J, Ribo M, Perren F, Saqqur M, Rubiera M, Sergentanis TN, Vadikolias K, Larrue V, Molina CA, Alexandrov AV. Safety and efficacy of ultrasound-enhanced thrombolysis: a comprehensive review and meta-analysis of randomized and nonrandomized studies. *Stroke* 2010; **41**: 280–7.
17 Porter TR, Le Veen RF, Fox R, Kricsfeld A, Xie F. Thrombolytic enhancement with perfluorocarbon-exposed sonicated dextrose albumin microbubbles. *Am Heart J* 1996; **132**: 964–8.
18 Nishioka T, Luo H, Fishbein MC, Cercek B, Forrester JS, Kim CJ, Berglund H, Siegel RJ. Dissolution of thrombotic arterial occlusion by high intensity, low frequency ultrasound and dodecafluoropentane emulsion: an in vitro and in vivo study. *J Am Coll Cardiol* 1997; **30**: 561–8.
19 Wu Y, Unger EC, McCreery TP, Sweitzer RH, Shen D, Wu G, Vielhauer MD. Binding and lysing of blood clots using MRX-408. *Invest Radiol* 1998; **33**: 880–5.
20 Xie F, Lof J, Matsunaga T, Zutshi R, Porter TR. Diagnostic ultrasound combined with glycoprotein IIb/IIIa-targeted microbubbles improves microvascular recovery after acute coronary thrombotic occlusions. *Circulation* 2009; **119**: 1378–85.
21 Birnbaum Y, Luo H, Nagai T, Fishbein MC, Peterson TM, Li S, Kricsfeld D, Porter TR, Siegel RJ. Noninvasive in vivo clot dissolution without a thrombolytic drug: recanalization of thrombosed iliofemoral arteries by transcutaneous ultrasound combined with intravenous infusion of microbubbles. *Circulation* 1998; **97**: 130–4.
22 Culp WC, Porter TR, Lowery J, Xie F, Roberson PK, Marky L. Intracranial clot lysis with intravenous microbubbles and transcranial ultrasound in swine. *Stroke* 2004; **35**: 2407–11.
23 Culp WC, Flores R, Brown AT, Lowery JD, Roberson PK, Hennings LJ, Woods SD, Hatton JH, Culp BC, Skinner RD, Borrelli MJ. Successful microbubble sonothrombolysis without tissue-type plasminogen activator in a rabbit model of acute ischemic stroke. *Stroke* 2011; **42**: 2280–5.
24 Porter TR, Xie F. Can transcranial ultrasound and microbubble therapy ever enter the mainstream in acute stroke therapy? *Expert Rev Cardiovasc Ther* 2012; **10**: 549–51.
25 Alexandrov AV, Mikulik R, Ribo M, Sharma VK, Lao AY, Tsivgoulis G, Sugg RM, Barreto A, Sierzenski P, Malkoff MD, Grotta JC. A pilot randomized clinical safety study of sonothrombolysis augmentation with ultrasound-activated perflutren–lipid microspheres for acute ischemic stroke. *Stroke* 2008; **39**: 1464–9.
26 Molina CA, Ribo M, Rubiera M, Montaner J, Santamarina E, Delgado-Mederos R, Arenillas JF, Huertas R, Purroy F, Delgado P, Alvarez-Sabín J. Microbubble administration accelerates clot lysis during continuous 2-MHz ultrasound monitoring in stroke patients treated with intravenous tissue plasminogen activator. *Stroke* 2006; **37**: 425–9.
27 Molina CA, Barreto AD, Tsivgoulis G, Sierzenski P, Malkoff MD, Rubiera M, Gonzales N, Mikulik R, Pate G, Ostrem J, Singleton W, Manvelian G, Unger EC, Grotta JC, Schellinger PD, Alexandrov AV. Transcranial ultrasound in clinical sonothrombolysis (TUCSON) trial. *Ann Neurol* 2009; **66**: 28–38.
28 Hagisawa K, Nishioka T, Suzuki R, Takizawa T, Maruyama K, Takase B, Ishihara M, Kurita A, Yoshimoto N, Ohsuzu F, Kikuchi M. Enhancement of ultrasonic thrombus imaging using bubble liposomes containing perfluorocarbon targeted to activated platelet glycoprotein IIb/IIIa complex in a rabbit iliac artery. *Int J Cardiol* 2011; **152**: 202–6.
29 *Instruction Manual of AC Calorimetric Thermal Constant Measuring System.* Yokohama, Japan: Sinku-Riko Inc., 1992.
30 Salazar AE. Experimental myocardial infarction. Induction of coronary thrombosis in the intact closed-chest dog. *Circ Res* 1961; **9**: 1351–6.
31 TIMI Study Group. The Thrombolysis in Myocardial Infarction (TIMI) trial: Phase I findings. *N Engl J Med* 1985; **312**: 932–6.
32 Daffertshofer M, Gass A, Ringleb P, Sitzer M, Sliwka U, Els T, Sedlaczek O, Koroshetz WJ, Hennerici MG. Transcranial low-frequency ultrasound-mediated thrombolysis in brain ischemia: increased risk of hemorrhage with combined ultrasound and tissue plasminogen activator: results of a phase II clinical trial. *Stroke* 2005; **36**: 1441–6.
33 Alonso A, Dempfle CE, Della Martina A, Stroick M, Fatar M, Zohsel K, Allémann E, Hennerici MG, Meairs S. In vivo clot lysis of human thrombus with intravenous abciximab immunobubbles and ultrasound. *Thromb Res* 2009; **124**: 70–4.
34 Baron C, Aubry JF, Tanter M, Meairs S, Fink M. Simulation of intracranial acoustic fields in clinical trials of sonothrombolysis. *Ultrasound Med Biol* 2009; **35**: 1148–58.
35 Ahmadi F, McLoughlin IV, Chauhan S, ter-Haar G. Bio-effects and safety of low-intensity, low-frequency ultrasonic exposure. *Prog Biophys Mol Biol* 2012; **108**: 119–38.
36 Luo H, Fishbein MC, Bar-Cohen Y, Nishioka T, Berglund H, Kim CJ, Nagai T, Birnbaum Y, Siegel RJ. Cooling system permits effective transcutaneous ultrasound clot lysis in vivo without skin damage. *J Thromb Thrombolysis* 1998; **6**: 125–31.
37 Storm G, Oussoren C, Peelers PAM, Barenholz Y. Tolerability of liposomes in vivo. In: Gregoriadis G, ed. *Liposome Technology*. Boca Raton, FL: CRC Press, 1993: 345–83.
38 Carpenter CP, Woodside MD, Kinkead ER, King JM, Sullivan LJ. Response of dogs to repeated intravenous injection of polyethylene glycol 4000 with notes on excretion and sensitization. *Toxicol Appl Pharmacol* 1971; **18**: 35–40.
39 Lee TY, Lin CT, Kuo SY, Chang DK, Wu HC. Peptide-mediated targeting to tumor blood vessels of lung cancer for drug delivery. *Cancer Res* 2007; **67**: 10958–65.
40 Chang DK, Lin CT, Wu CH, Wu HC. A novel peptide enhances therapeutic efficacy of liposomal anticancer drugs in mice models of human lung cancer. *PLoS ONE* 2009; **4**: e4171.
41 Wei K, Mulvagh SL, Carson L, Davidoff R, Gabriel R, Grimm RA, Wilson S, Fane L, Herzog CA, Zoghbi WA, Taylor R, Farrar M, Chaudhry FA, Porter TR, Irani W, Lang RM. The safety of Definity and Optison for ultrasound image enhancement: a retrospective analysis of 78,383 administered contrast doses. *J Am Soc Echocardiogr* 2008; **11**: 1202–6.
42 Hutter JC, Luu HM, Mehlhaff PM, Killam AL, Dittrich HC. Physiologically based pharmacokinetic model for fluorocarbon elimination after the administration of an octafluoropropane–albumin microsphere sonographic contrast agent. *J Ultrasound Med* 1999; **18**: 1–11.

Ultrasound-Mediated Gene Delivery Systems by AG73-Modified Bubble Liposomes

Yoichi Negishi,[1] Yuka Tsunoda,[1] Nobuhito Hamano,[1] Daiki Omata,[2] Yoko Endo-Takahashi,[1] Ryo Suzuki,[2] Kazuo Maruyama,[2] Motoyoshi Nomizu,[3] Yukihiko Aramaki[1]

[1]*Department of Drug Delivery and Molecular Biopharmaceutics, School of Pharmacy, Tokyo University of Pharmacy and Life Sciences, Hachioji, Tokyo, Japan*

[2]*Laboratory of Drug and Gene Delivery, Faculty of Pharma-Sciences, Teikyo University, Tokyo, Japan*

[3]*Department of Clinical Biochemistry, School of Pharmacy, Tokyo University of Pharmacy and Life Sciences, Hachioji, Tokyo, Japan*

Received 1 February 2013; revised 11 March 2013; accepted 17 March 2013
Published online 19 July 2013 in Wiley Online Library (wileyonlinelibrary.com). DOI 10.1002/bip.22246

ABSTRACT:

Targeted gene delivery to neovascular vessels in tumors is considered a promising strategy for cancer therapy. We previously reported that "Bubble liposomes" (BLs), which are ultrasound (US) imaging gas-encapsulating liposomes, were suitable for US imaging and gene delivery. When BLs are exposed to US, the bubble is destroyed, creating a jet stream by cavitation, and resulting in the instantaneous ejection of extracellular plasmid DNA (pDNA) or other nucleic acids into the cytosol. We developed AG73 peptide-modified Bubble liposomes (AG73-BL) as a targeted US contrast agent, which was designed to attach to neovascular tumor vessels and to allow specific US detection of angiogenesis (Negishi et al., Biomaterials 2013, 34, 501–507). In this study, to evaluate the effectiveness of AG73-BL as a gene delivery tool for neovascular vessels, we examined the gene transfection efficiency of AG73-BL with US exposure in primary human endothelial cells (HUVEC). The transfection efficiency was significantly enhanced if the AG73-BL attached to the HUVEC was exposed to US compared to the BL-modified with no peptide or scrambled peptide. In addition, the cell viability was greater than 80% after transfection with AG73-BL. These results suggested that after the destruction of the AG73-BL with US exposure, a cavitation could be effectively induced by the US exposure against AG73-BL binding to the cell surface of the HUVEC, and the subsequent gene delivery into cells could be enhanced. Thus, AG73-BL may be useful for gene delivery as well as for US imaging of neovascular vessels.

Keywords: AG73; Bubble liposome; gene delivery; syndecan; ultrasound imaging

This article was originally published online as an accepted preprint. The "Published Online" date corresponds to the preprint version. You can request a copy of the preprint by emailing the Biopolymers editorial office at biopolymers@wiley.com

INTRODUCTION

Gene therapy is expected as a potential alternative to conventional therapeutic approach. However, safe and effective gene delivery techniques are required to realize its clinical application. Recently, among the various attempts to develop clinically applicable gene therapy, despite their relatively lower efficiency, nonviral

Yoichi Negishi and Yuka Tsunoda contributed equally to this work.
Correspondence to: Yoichi Negishi, Department of Drug Delivery and Molecular Biopharmaceutics, School of Pharmacy, Tokyo University of Pharmacy and Life Sciences, Hachioji, Tokyo, Japan; e-mail: negishi@toyaku.ac.jp
Contract grant sponsor: Industrial Technology Research Grant Program from New Energy, Industrial Technology Development Organization (NEDO) of Japan
Contract grant number: 04A05010
Contract grant sponsor: Grant-in-Aid for Exploratory Research
Contract grant number: 18650146
Contract grant sponsor: Grant-in-Aid for Scientific Research (B) from the Japan Society of the Promotion of Science of Japan
Contract grant number: 20300179

methods are focused on safer alternatives in gene therapy to viral vectors. Among nonviral physical delivery methods,[1–4] it has been shown that ultrasound (US) exposure enhances the efficiency of drug or gene delivery into tissues and cells, a technique known as sonoporation.[3] It is believed that this effect transiently increases the permeability of cell membranes around by US cavitation activity, enabling the transport of extracellular molecules into viable cells.[2,5–8] Microbubbles can act as contrast agents for US imaging by enabling visualization of disease site and enhancing the delivery efficiency of drugs or genes by cavitation as a result of US exposure while reducing cellular damage.[9–15] Conventional microbubbles containing US echo-contrast gases are commercially available.[16,17] However, these microbubbles exhibit problems with size, stability, and targeting function. Liposomes—useful carriers of drugs, antigens, and genes—can easily be prepared in a variety of sizes and modified to add a targeting function.[18–22] Therefore, we assumed that polyethylene glycol-modified liposomes containing the US imaging gas (*perfluoropropane gas*) could be novel gene delivery carriers. We have previously developed novel liposomal bubbles, "Bubble liposomes" (BLs), which could solve the problems faced with microbubbles and which could feasibly be used for delivering genes in vitro and in vivo.[17,23–28]

There is currently a need for imaging angiogenesis both for diagnostic purposes and for assessing therapeutic effects. Targeted contrast US provides an opportunity when moieties such as peptides or monoclonal antibodies that bind to the endothelial cell surface are utilized to image angiogenesis.

Many types of peptides have been reported that specifically bind to tumor angiogenic endothelium, including the AG73 peptide, which is considered a ligand for syndecan.[29–32] Moreover, syndecan-2 is highly expressed in neovascular vessels.[33–36] We hypothesized that BLs targeted via linkage with AG73 would specifically adhere to the tumor angiogenic endothelium, and this selective adhesion would allow us to detect tumor angiogenesis ultrasonically. We have recently succeeded in developing AG73-modified BLs (AG73-BL) as a targeted US contrast agent.[37] If the AG73-BL is used for gene delivery in combination with US exposure, efficient cavitation may be induced at the surface of the target cells, leading to the delivery of extracellular pDNA into the cytosol. However, it is unknown whether a gene delivery system with the combination of AG73-BL and US exposure will be an effective method. Herein, we assessed the gene delivery ability of AG73-BL to HUVEC as a component cell of blood vessels.

MATERIALS AND METHODS

Materials

Dipalmitoylphosphatidylcholine (DPPC), 1,2-distearoylphosphatidylethanolamine-methoxy-polyethyleneglycol (DSPE-PEG_{2000}-OMe), and 1,2-distearoyl-*sn*-glycero-3-phosphatidylethanolamine-polyethyleneglycol-maleimide (DSPE-PEG_{2000}-Mal) were purchased from NOF Corporation (Tokyo, Japan). An Endothelial Cell Growth Medium Kit was purchased from Cell Applications, Inc. (San Diego, CA). All other materials were used without further purification.

Preparation of Liposomes and BLs

To prepare liposomes for the BLs, DPPC and DSPE-PEG_{2000}-OMe were mixed at a molar ratio of 94:6. The liposomes were prepared by a reverse-phase evaporation method, as described previously.[23,24] In brief, all the reagents were dissolved in 1:1 (v/v) chloroform/diisopropylether. Phosphate-buffered saline was added to the lipid solution, and the mixture was sonicated and then evaporated at 47°C. The organic solvent was completely removed, and the size of the liposomes was adjusted to less than 200 nm using extrusion equipment and a sizing filter (Nuclepore Track-Etch Membrane, 200 nm pore size, Whatman plc, UK). After being sized, the liposomes were passed through a sterile 0.45-μm syringe filter (Asahi Technoglass, Chiba, Japan) for sterilization. For the fluorescent labeling of the lipid membrane,1,1-dioctadecyl-3,3,3,3-tetramethyl-indocarbocyanine perchlorate (DiI: 0.1 or 1 mol% of total lipids) was added. The lipid concentration was measured using the Phospholipid C test (Wako Pure Chemical Industries, Osaka, Japan). BLs were prepared from liposomes and perfluoropropane gas (Takachiho Chemical, Tokyo, Japan). First, 5 mL sterilized vials containing 2 mL of a liposome suspension (lipid concentration: 1 mg/mL) were filled with perfluoropropane gas, capped, and pressurized with 7.5 mL of perfluoropropane gas. The vials were placed in a bath-type sonicator (42 kHz, 100 W, Bransonic 2510J-DTH, Branson Ultrasonics, Danbury, CT) for 5 min to form BL. The mean size of the BLs were determined using the light-scattering method with a zeta potential/particle sizer (Nicomp 380ZLS, Santa Barbara, CA). As shown in previous report, it was confirmed that the mean particle diameter of BLs ranged from 400 to 600 nm with a relatively narrow distribution after the encapsulation of the gas.[37]

Preparation of AG73 Peptide-Modified Liposomes and BLs

The Cys-AG73 peptide (CGG-RKRLQVQLSIRT) and a scrambled Cys-AG73T control peptide (CGG-LQQRRSVLRTKI) were synthesized manually using the 9-fluorenylmethoxycarbonyl (Fmoc)-based solid-phase strategy, prepared in the COOH terminal amide form, and purified by reverse-phase, high-performance liquid chromatography. The peptides were confirmed by an electrospray ionization mass spectrometer at the Central Analysis Center, Tokyo University of Pharmacy and Life Sciences. Liposomes composed of DPPC, DSPE-PEG_{2000}-OMe, and DSPE-PEG_{2000}-Mal at a molar ratio of 94:5.8:0.2 were prepared by a reverse-phase evaporation method. For the preparation of AG73 peptide-modified liposomes, adequate amounts of AG73 peptide were added to the liposomes and gently mixed, as described previously.[37] Briefly, for coupling, AG73 peptide at a molar ratio of fivefold DSPE-PEG_{2000}-Mal was added to the liposomes in the presence of tris(2-carboxyethyl)phosphine hydrochloride, and the mixture was incubated for 6 h at room temperature to conjugate the cysteine of the Cys-AG73 peptide with the maleimide of the liposomes through a thioether bond. The resulting AG73 peptide-conjugated liposomes (AG73-liposomes) were dialyzed to remove any excess

peptide. The AG73-liposomes were modified with 6 mol% PEG and 0.2 mol% peptides. AG73 peptide-modified BLs (AG73-BL) were prepared from liposomes and perfluoropropane gas. The conjugation of AG73 to PEG liposomes has been confirmed by reverse-phase high-performance liquid chromatography (HPLC) analysis as shown in our previous report.[38] Results showed that Cys-AG73 peptide could be completely conjugated to DSPE-PEG2000-Mal. The average number of the peptides per BL was approximately 30 peptide molecules based on the calculation by using the above values and the assumption that the molecular weight of peptide is 2000; the average number of phospholipid molecules per liposome was estimated by the method of Enoch and Strittmatter.[39]

Cell Lines

Human umbilical vein endothelial cells (HUVECs) were purchased from Cell Applications and cultured using an Endothelial Cell Growth Medium Kit. All experiments were performed using HUVECs between passage 5 and 9.

Microscopic Analyses

The day before transfection, HUVEC (3×10^4 cells/well) were seeded in the wells of a 48-well plate (Asahi Technoglass, Chiba, Japan) and incubated for 18 h at 37°C in 5% CO_2. Thirty micrograms of AG73-BL was mixed with the culture medium and added to the cells. The plates were sealed with sterile tape and inverted for 5 min. The images of the cells bound with the BL, AG73-BL, or AG73T-BL were randomly captured with a microscope (Axiovert 200 M, Carl Zeiss) at 100× magnification. Total number of bound bubbles per cell ($n = 300$ cells per each treatment) in four images was counted. Number of each bubbles binding to one HUVEC are averaged.

Plasmid DNA

The plasmid pcDNA3-Luc, derived from pGL3-basic (Promega, Madison, WI), is an expression vector encoding the firefly luciferase gene under the control of a cytomegalovirus promoter.

Transfection of pDNA Using BL, AG73-BL, or AG73T-BL

The day before transfection, HUVEC (3×10^4 cells/well) were seeded in the wells of a 48-well plate (Asahi Technoglass, Chiba, Japan) and incubated for 18 h at 37°C in 5% CO_2. Ten to thirty micrograms of BL, AG73-BL, or AG73T-BL and 14 μg of pDNA were mixed with the culture medium and added to the cells. The plates were sealed with sterile tape and inverted for 5 min. After the interaction between each type of BL and the cells, the tape was removed and the cells were immediately exposed to US (frequency, 2 MHz; duty, 50%; burst rate, 2.0 Hz; intensity, 0.1 W/cm^2) for 10 s through a 6-mm-diameter probe placed in the well. A Sonopore 3000 sonicator (NEPA GENE, Chiba, Japan) was used to generate the US. The cells were washed twice with culture medium and cultured for 2 days. For the measurement of luciferase expression, cell lysate was prepared with a lysis buffer (0.1*M* Tris-HCl (pH 7.8), 0.1% Triton X-100, and 2 m*M* EDTA). Luciferase activity was measured using a luciferase assay system (Promega, Madison, WI) and a luminometer (LB96V, Belthold Japan, Tokyo, Japan). The activity is indicated as relative light units (RLUs) per mg of protein.

Cytotoxicity of BL, AG73-BL, or AG73T-BL and US to HUVEC

One day after transfection as described above, cell viability was assayed using Cell Counting Kit-8 (Dojindo, Kumamoto, Japan). Briefly, WST-8 (10 μL) was added to each well and the cells were incubated at 37°C for 2 h. The formazan product was dissolved in 10 μL of HCl (0.1*M*) to stop the reaction. The color intensity was measured using a microplate reader at test and reference wavelengths of 450 and 650 nm, respectively.

Statistical Analyses

All data are shown as mean $\pm$ SD ($n = 4$). The data were considered significant when $P < 0.05$. The *t*-test was used to calculate statistical significance.

RESULTS AND DISCUSSION

Adhesion of AG73 Peptide-Modified Bubble Liposomes (AG73-BL) to HUVECs

As shown in Figure 1, if BLs modified with a targeting ligand are prepared and used for gene delivery in combination with US exposure, after the binding of the BL onto the target cell and exposure to US, it is possible that efficient cavitation will occur just above the target cell membrane, leading to efficient gene delivery into the target cell. Indeed, we observed that gene delivery could be significantly enhanced when culture plate with adherence cell lines (HUVEC or COS7 cells) were mixed with the solution of BLs and pDNA, inverted for several minutes, and exposed to US (data not shown). In this situation, it is possible that BLs can be easily accessible to the surface of cell membrane because of the floating character of itself. Therefore, these results may suggest that destruction and cavitation of BLs by US exposure occur on the surface of cell membrane, leading to more efficient gene delivery.

More recently, we have developed AG73 peptide-modified Bubble liposomes (AG73-BL) as neovascular-targeting BLs to enhance the contrast image.[37] Therefore, we assumed that AG73-BL in combination with US exposure could induce cavitation directly above the target cell membrane. Prior to the transfection experiment using the AG73-BL, we first confirmed the adhesion of AG73-BL to HUVECs as a component cell of blood vessels in the culture plate. To confirm whether AG73-BL actually bind to the surface of HUVECs in the culture plate, AG73-BL was mixed with the culture medium and added to the cells. The plates were deaerated with the mixture, sealed with sterile tape, and inverted for 5 min to float and attach the AG73-BL onto the cell membranes. Then, the cells were observed under a microscope. As shown in Figure 2, we found that AG73-BL could bind to the cells. In contrast, nonlabeled BL (BL) or scrambled peptide-modified BLs (AG73T-BL) had

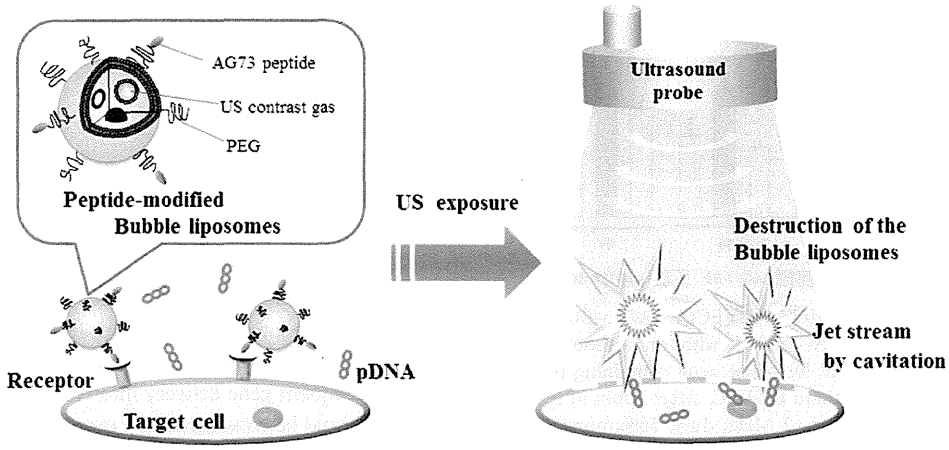

FIGURE 1 Scheme of gene transfection with AG73-BLs exposed to US. If AG73 peptide-modified BL, which can attach to the cell membrane of HUVECs, is used for gene delivery in combination with US exposure, after binding the AG73-BL onto the cell membrane of the HUVECs and exposing it to US, it may be possible for efficient cavitation to be induced on the target cell membrane, leading to efficient gene delivery into the target cell.

very low affinity for binding to the cells. The AG73 peptide is derived from laminin and serves as a ligand for syndecans, which are highly expressed on HUVECs.[35,36] The AG73 peptide also binds to the heparan sulfate side chains of syndecans.[30,31] Therefore, these results suggested that AG73-BL could effectively bind to HUVECs via the syndecan receptor.

Gene Transfection by the Combination of AG73-BL and US Exposure

Using luciferase-expressing pDNA to assess the gene delivery efficiency, we examined the gene delivery capacity of the AG73-BL into the cells in the combination with US exposure. As shown in Figure 3, highly efficient gene expression was observed when the AG73-BL and US exposure were applied. In contrast, lower gene expression was observed with the use of BL or AG73T-BL. We found that the cavitation induction on the cell surface by the combination of AG73-BL and US exposure was important in achieving efficient gene delivery. The cytotoxicity of the combination of AG73-BL and US exposure was determined using the WST assay. However, cell viability was more than 80% after each transfection (Figure 4). These results suggest that the AG73-BL has stronger adherence to the cells compared to BL or AG73T-BL, which lead to the inducement of efficient cavitation on the cell membrane and the delivery of plasmid DNA into the cells. In the case of systemic gene delivery, transfection efficiency is decreased if the BL and gene are not colocalized in blood vessels. Therefore, it is necessary to control the biodistribution of both the BL and the gene, and to consider the degradation of the gene by nuclease. To overcome these problems, we have developed plasmid DNA and siRNA-loaded Bubble liposomes containing cationic lipids that are capable of loading plasmid DNA or siRNA.[40–42] We

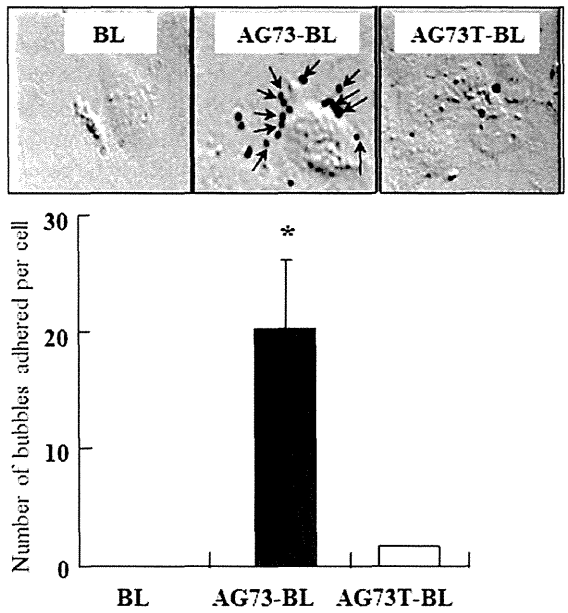

FIGURE 2 Comparison of the cell attachment properties of BL, AG73-BL, or AG73T-BL by microscopic analysis. BL, AG73-BL, or AG73T-BL was added to each HUVEC culture. After 5 min of incubation, each specimen was observed with bright field microscopy. The binding bubbles to HUVEC are indicated by arrows. Magnification: ×100. The number of bubbles binding to one HUVEC is measured. $^*P < 0.05$ compared with AG73T-BL or BL.

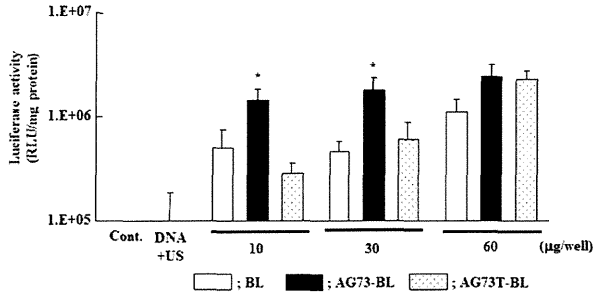

FIGURE 3 Gene transfection into HUVECs by AG73-BL and US exposure. BL, AG73-BL, or AG73T-BL with or without pDNA (CMV promoter/enhancer and luciferase gene containing plasmid DNA) was added to each cultured HUVEC. After 5 min of incubation, US was applied (frequency, 2 MHz; duty, 50%; burst rate, 2 Hz; intensity, 0.1 W/cm^2; time, 10 s). The cells were cultured for 48 h, and luciferase activity was determined. $^*P < 0.05$ compared with AG73T-BL or BL.

have also reported that newly developed AG73-BL can work as an US imaging agent that targets tumor vessels and allows imaging in in vivo studies.[37] Therefore, if AG73-BLs containing cationic lipids are prepared, they could become an ideal US-responsive and neovasculature-selective gene delivery tool when used in combination with US exposure and could lead to beneficial clinical applications for cancer therapy.

Recently, the term theranostics has been defined as a combined method of the modalities of diagnostic imaging and therapy, which enables simultaneous diagnosis and delivery of therapeutic drugs or genes.[43] Therefore, if BLs with cationic lipids are encapsulated with an echo-contrast gas, modified with a targeting ligand, and loaded with a therapeutic gene, the combination with US may enable target-tissue specific US imaging and gene therapy by the theranostic approach.

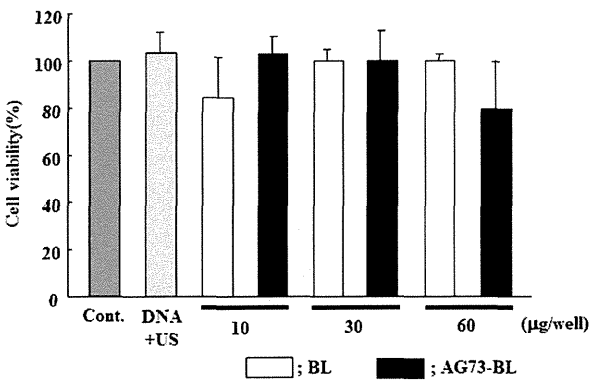

FIGURE 4 Cytotoxicity of BL or AG73-BL with US exposure. BL or AG73-BL was added to each cultured HUVEC. After 5 min of incubation, US was applied (frequency, 2 MHz; duty, 50%; burst rate, 2 Hz; intensity, 0.1 W/cm^2; time, 10 s). The cytotoxicity 1 day after transfection by the combination of AG73-BL and US exposure was determined using the WST assay. All data represent the mean ± SD (n = 4).

CONCLUSIONS

In this study, we showed that AG73-BL could stably and specifically attach onto the surface of HUVECs via a ligand for syndecans. Furthermore, the gene delivery efficiency was higher than that of control BL (nonlabeled BL or AG73T-BL), when US exposure was applied after the attachment. These results suggested that cavitation could be effectively induced by US exposure to AG73-BL binding to the cell surface of HUVECs, and the subsequent gene delivery into cells could be enhanced. AG73-BL should be considered as a more feasible gene delivery tool and an US contrast agents in vivo. Therefore, the combination of AG73-BL and US exposure may be useful for US imaging and the delivery of pDNA or other nucleic acid molecules to the neovasculature in tumors via systemic injection and may be applicable to a less invasive diagnostic and therapeutic system.

We are grateful to Dr. Katsuro Tachibana (Department of Anatomy, School of Medicine, Fukuoka University) for technical advice regarding the induction of cavitation with US and Mr. Yasuhiko Hayakawa and Mr. Kosho Suzuki (NEPA GENE CO., LTD.) for technical advice regarding exposure to US.

REFERENCES

1. Neumann, E.; Schaefer-Ridder, M.; Wang, Y.; Hofschneider, P. H. EMBO J 1982, 1, 841–845.
2. Greenleaf, W. J.; Bolander, M. E.; Sarkar, G.; Goldring, M. B.; Greenleaf, J. F. Ultrasound Med Biol 1998, 24, 587–595.
3. Fechheimer, M.; Boylan, J. F.; Parker, S.; Sisken, J. E.; Patel, G. L.; Zimmer, S. G. Proc Natl Acad Sci USA 1987, 84, 8463–8467.
4. Liu, F.; Song, Y.; Liu, D. Gene Ther 1999, 6, 1258–1266.
5. Delius, M.; Adams, G. Cancer Res 1999, 59, 5227–5232.
6. Duvshani-Eshet, M.; Machluf, M. J Control Release 2005, 108, 513–528.
7. Holmes, R. P.; Yeaman, L. D.; Taylor, R. G.; McCullough, D. L. J Urol 1992, 147, 733–737.
8. Schratzberger, P.; Krainin, J. G.; Schratzberger, G.; Silver, M.; Ma, H.; Kearney, M.; Zuk, R. F.; Brisken, A. F.; Losordo, D. W.; Isner, J. M. Mol Ther 2002, 6, 576–583.
9. Kinoshita, M.; Hynynen, K. Biochem Biophys Res Commun 2005, 335, 393–399.
10. Li, T.; Tachibana, K.; Kuroki, M.; Kuroki, M.; Radiology 2003, 229, 423–428.
11. Sonoda, S.; Tachibana, K.; Uchino, E.; Okubo, A.; Yamamoto, M.; Sakoda, K.; Hisatomi, T.; Sonoda, K. H.; Negishi, Y.; Izumi, Y.; Takao, S.; Sakamoto, T. Invest Ophthalmol Vis Sci 2006, 47, 558–564.
12. Taniyama, Y.; Tachibana, K.; Hiraoka, K.; Aoki, M.; Yamamoto, S.; Matsumoto, K.; Nakamura, T.; Ogihara, T.; Kaneda, Y.; Morishita, R. Gene Ther 2002, 9, 372–380.

13. Taniyama, Y.; Tachibana, K.; Hiraoka, K.; Namba, T.; Yamasaki, K.; Hashiya, N.; Aoki, M.; Ogihara, T.; Yasufumi, K.; Morishita, R. Circulation 2002, 105, 1233–1239.
14. Tsunoda, S.; Mazda, O.; Oda, Y.; Iida, Y.; Akabame, S.; Kishida, T.; Shin-Ya, M.; Asada, H.; Gojo, S.; Imanishi, J.; Matsubara, H.; Yoshikawa, T. Biochem Biophys Res Commun 2005, 336, 118–127.
15. Unger, E. C.; Porter, T.; Culp, W.; Labell, R.; Matsunaga, T.; Zutshi, R. Adv Drug Deliv Rev 2004, 56, 1291–1314.
16. Lindner, J. R. Nat Rev Drug Discov 2004, 3, 527–532.
17. Suzuki, R.; Takizawa, T.; Negishi, Y.; Utoguchi, N.; Maruyama, K. Int J Pharm 2008, 354, 49–55.
18. Allen, T. M.; Hansen, C.; Martin, F.; Redemann, C.; Yau-Young, A. Biochim Biophys Acta 1991, 1066, 29–36.
19. Blume, G.; Cevc, G. Biochim Biophys Acta 1990, 1029, 91–97.
20. Harata, M.; Soda, Y.; Tani, K.; Ooi, J.; Takizawa, T.; Chen, M.; Bai, Y.; Izawa, K.; Kobayashi, S., Tomonari, A.; Nagamura, F.; Takahashi, S.; Uchimaru, K.; Iseki, T.; Tsuji, T.; Takahashi, T. A.; Sugita, K.; Nakazawa, S.; Tojo, A.; Maruyama, K.; Asano, S. Blood 2004, 104, 1442–1449.
21. Maruyama, K.; Ishida, O.; Kasaoka, S.; Takizawa, T.; Utoguchi, N.; Shinohara, A.; Chiba, M.; Kobayashi, H.; Eriguchi, M.; Yanagie, H. J Control Release 2004, 98, 195–207.
22. Maruyama, K.; Yuda, T.; Okamoto, A.; Kojima, S.; Suginaka, A.; Iwatsuru, M. Biochim Biophys Acta 1992, 1128, 44–49.
23. Suzuki, R.; Takizawa, T.; Negishi, Y.; Hagisawa, K.; Tanaka, K.; Sawamura, K.; Utoguchi, N.; Nishioka, T.; Maruyama, K. J Control Release 2007, 117, 130–136.
24. Negishi, Y.; Endo, Y.; Fukuyama, T.; Suzuki, R.; Takizawa, T.; Omata, D.; Maruyama, K.; Aramaki, Y. J Control Release 2008, 132, 124–130.
25. Suzuki, R.; Takizawa, T.; Negishi, Y.; Utoguchi, N.; Sawamura, K.; Tanaka, K.; Namai, E.; Oda, Y.; Matsumura, Y.; Maruyama, K. J Control Release 2008, 125, 137–144.
26. Negishi, Y.; Tsunoda, Y.; Endo-Takahashi, Y.; Oda, Y.; Suzuki, R.; Maruyama, K.; Yamamoto, M.; Aramaki, Y. J Drug Delivery 2011, 2011, 203986.
27. Negishi, Y.; Matsuo, K.; Endo-Takahashi, Y.; Suzuki, K.; Matsuki, Y.; Takagi, N.; Suzuki, R.; Maruyama, K.; Aramaki, Y. Pharm Res 2011, 28, 712–719.
28. Sugano, M.; Negishi, Y.; Endo-Takahashi, Y.; Suzuki, R.; Maruyama, K.; Yamamoto, M.; Aramaki, Y. Int J Pharm 2012, 422, 332–337.
29. Carey, D. J. Biochem J 1997, 327, 1–16.
30. Hoffman, M. P.; Nomizu, M.; Roque, E.; Lee, S.; Jung, D. W.; Yamada, Y.; Kleinman, H. K. J Biol Chem 1998, 273, 28633–28641.
31. Nomizu, M.; Kuratomi, Y.; Malinda, K. M.; Song, S. Y.; Miyoshi, K.; Otaka, A.; Powell, S. K.; Hoffman, M. P.; Kleinman, H. K.; Yamada, Y. J Biol Chem 1998, 273, 32491–32499.
32. Suzuki, N.; Ichikawa, N.; Kasai, S.; Yamada, M.; Nishi, N.; Morioka, H.; Yamashita, H.; Kitagawa, Y.; Utani, A.; Hoffman, M. P.; Nomizu, M. Biochemistry 2003, 42, 12625–12633.
33. Couchman, J. R. Nat Rev Mol Cell Biol 2003, 4, 926–937.
34. Fears, C. Y.; Gladson, C. L.; Woods, A. J Biol Chem 2006, 281, 14533–14536.
35. Halden, Y.; Rek, A.; Atzenhofer, W.; Szilak, L.; Wabnig, A.; Kungl, A. J. Biochem J 2004, 377 (Part 2), 533–538.
36. Mertens, G.; Cassiman, J. J.; Van den Berghe, H.; Vermylen, J.; David, G. J Biol Chem 1992, 267, 20435–20443.
37. Negishi, Y.; Hamano, N.; Tsunoda, Y.; Oda, Y.; Choijamts, B.; Endo-Takahashi, Y.; Omata, D.; Suzuki, R.; Maruyama, K.; Nomizu, M.; Emoto, M.; Aramaki, Y. Biomaterials 2013, 34, 501–507.
38. Negishi, Y.; Omata, D.; Iijima, H.; Hamano, N.; Endo-Takahashi, Y.; Nomizu, M.; Aramaki, Y. Biol Pharm Bull 2010, 33, 1766–17691.
39. Enoch, H.; Strittmatter, P. Proc Natl Acad Sci USA 1979, 76, 145–149.
40. Negishi, Y.; Endo-Takahashi, Y.; Matsuki, Y.; Kato, Y.; Takagi, N.; Suzuki, R.; Maruyama, K.; Aramaki, Y. Mol Pharm 2012, 9, 1834–1840.
41. Endo-Takahashi, Y.; Negishi, Y.; Kato, Y.; Suzuki, R.; Maruyama, K.; Aramaki, Y. Int J Pharm 2012, 422, 504–509.
42. Endo-Takahashi, Y.; Negishi, Y.; Nakamura, A.; Suzuki, D.; Ukai, S.; Sugimoto, K.; Moriyasu, F.; Takagi, N.; Suzuki, R.; Maruyama, K.; Aramaki, Y. Biomaterials 2013, 34, 2807–2813.
43. Sumer, B.; Gao, J. Nanomedicine (Lond) 2008, 3, 137–140.

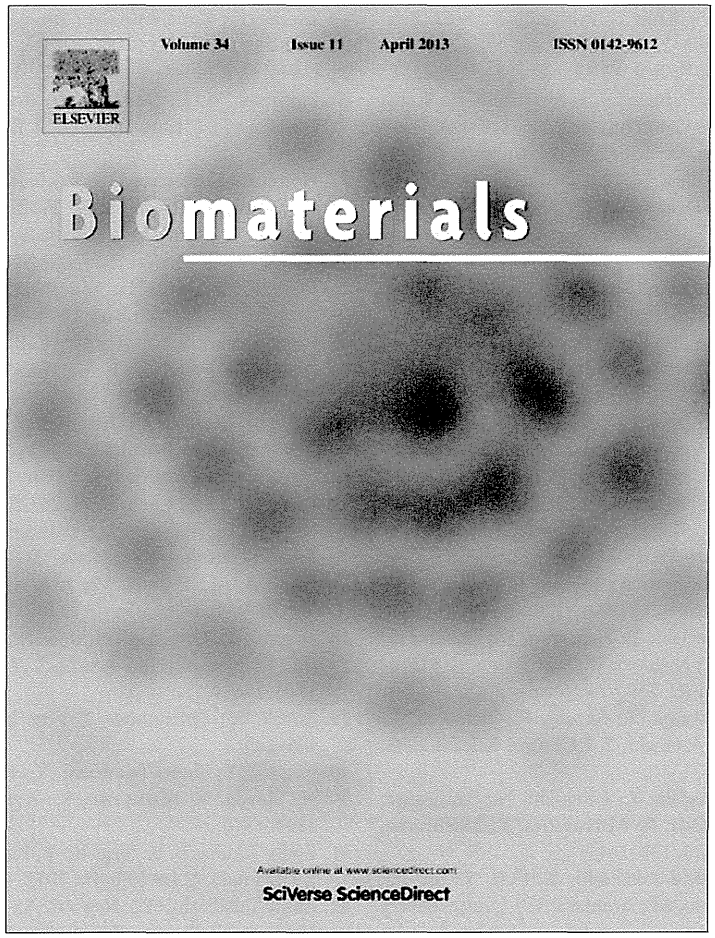

Biomaterials 34 (2013) 2807–2813

Contents lists available at SciVerse ScienceDirect

Biomaterials

journal homepage: www.elsevier.com/locate/biomaterials

pDNA-loaded Bubble liposomes as potential ultrasound imaging and gene delivery agents

Yoko Endo-Takahashi [a], Yoichi Negishi [a,*], Arisa Nakamura [a], Daichi Suzuki [a], Saori Ukai [a], Katsutoshi Sugimoto [b], Fuminori Moriyasu [b], Norio Takagi [c], Ryo Suzuki [d], Kazuo Maruyama [d], Yukihiko Aramaki [a]

[a] Department of Drug Delivery and Molecular Biopharmaceutics, School of Pharmacy, Tokyo University of Pharmacy and Life Sciences, 1432-1 Horinouchi, Hachioji, Tokyo 192-0392, Japan
[b] Department of Gastroenterology and Hepatology, Tokyo Medical University, 6-7-1 Nishishinjuku, Shinjuku-ku, Tokyo 160-0023, Japan
[c] Department of Molecular and Cellular Pharmacology, School of Pharmacy, Tokyo University of Pharmacy and Life Sciences, 1432-1 Horinouchi, Hachioji, Tokyo 192-0392, Japan
[d] Laboratory of Drug and Gene Delivery, Faculty of Pharma Sciences, Teikyo University, 2-11-1 Kaga, Itabashi-ku, Tokyo 173-8605, Japan

ARTICLE INFO

Article history:
Received 22 November 2012
Accepted 15 December 2012
Available online 21 January 2013

Keywords:
Bubble liposomes
Cationic lipid
Ultrasound imaging
Gene delivery

ABSTRACT

We have developed polyethyleneglycol (PEG)-modified liposomes (Bubble liposomes; BLs) that entrap ultrasound (US) contrast gas, and we have reported that the combination of BLs and US exposure was an effective tool for delivering pDNA and siRNA *in vitro* and *in vivo*. In this study, we prepared pDNA-loaded BLs using three types of cationic lipids to enhance the US imaging effect and the transfection efficiency via systemic injection. We investigated the US imaging abilities of these BLs, their protective effects on pDNA from serum component, and their transfection effects *in vitro* and *in vivo*. As a result, we demonstrated that the US imaging ability and transfection effect varied with lipid component and that p-BLs containing DSDAP could be the most stable and effective tool the among three types of p-BLs. Indeed, in ischemic muscle, p-BLs containing DSDAP could be detected using diagnostic US and could deliver bFGF-expressing pDNA using therapeutic US, leading to the induction of angiogenic factors and the improvement of blood flow. These results suggest that combining p-BLs with US exposure may be useful for stable US imaging and efficient gene delivery and may lead to the establishment of a theranostic approach, which is a combination of disease diagnosis and therapy.

1. Introduction

Various techniques using nanoparticles in combination with light, sound, and electromagnetic fields are currently being developed for both therapeutic and diagnostic application [1–9]. The term theranostic describes technology with concurrent and complementary diagnostic and therapeutic capabilities. Among all diagnostic imaging techniques, ultrasound (US) imaging has a unique advantage because it is real-time, low-cost, safe, and easy to incorporate into portable devices. In fact, US is used widely in clinical settings not only for diagnosis but also for therapy. With the use of microbubbles as US contrast agents the sensitivity of US imaging has been greatly improved. Furthermore, a combination of US and microbubbles has been proposed as a less invasive and tissue-specific method for gene delivery. This combination produces transient changes in the permeability of the cell membrane and allows for the site-specific, intracellular delivery of molecules such as dextran, pDNA, siRNA, and peptides both *in vitro* and *in vivo* [10–15].

Microbubbles hold significant potential for theranostic applications, given their propensity to be visualized *in vivo* with high sensitivity, their ability to improve drug delivery across biologic barriers, and the possibility of loading therapeutic molecules into or onto their shell. However, microbubbles have room for improvement in size, stability, and targeting function. To solve these issues, we previously developed "Bubble liposomes" (BLs). These are PEG-modified liposomes that contain echo-contrast gas, which can function as a gene and siRNA delivery tool with US exposure *in vitro* and *in vivo* [16–20]. Furthermore, to increase the efficiency of nucleic acid delivery via systemic injection, we prepared pDNA-loaded BLs (p-BLs) and siRNA-loaded BLs (si-BLs) using 1,2-dioleoyl-3-trimethylammonium-propane (DOTAP), a cationic lipid often used for gene delivery [21,22]. These types of BLs could improve the stability of nucleic acids in the presence of serum so that the effects of nucleic acid delivery can be observed.

* Corresponding author. Tel./fax: +81 42 676 3183.
E-mail address: negishi@toyaku.ac.jp (Y. Negishi).

0142-9612/$ – see front matter © 2013 Elsevier Ltd. All rights reserved.
http://dx.doi.org/10.1016/j.biomaterials.2012.12.018

In this study, we attempted to develop p-BLs that have the potential to be useful contrast agents and efficient delivery tools for gene therapy. We examined the therapeutic effect of gene delivery using the hindlimb ischemia mouse model.

2. Materials and methods

2.1. Preparation of liposomes and BLs

To prepare liposomes for BLs that do not contain cationic lipid, 1,2-dipalmitoyl-sn-glycero-phosphatidylcholine (DPPC) and 1,2-distearoylphosphatidylethanolamine-methoxy-polyethylene glycol (PEG_{2000}) were mixed at a molar ratio of 94:6. Both lipids were purchased from NOF Corporation (Tokyo, Japan). For BLs containing cationic lipid, 1,2-stearoyl-3-trimethylammonium-propane (DSTAP), 1,2-distearoyl-3-dimethylammonium-propane (DSDAP), and dimethyldioctadecylammonium bromide (DDAB) from Avanti Polar Lipids (Alabaster, AL) were used. Liposomes with various lipid compositions were prepared using the reverse phase evaporation method as described previously [19]. Briefly, DPPC, cationic lipid, and PEG_{2000} were mixed at a molar ratio of 64:30:6 and dissolved in 1:1 (*v/v*) chloroform/diisopropylether. HEPES-buffered saline (HBS: 150 mM NaCl, 10 mM HEPES, pH 7.0) was added to the lipid solution, and the mixture was sonicated and then evaporated. The organic solvent was completely removed, and the size of the liposomes was adjusted to less than 200 nm using extruding equipment and a sizing filter (Nuclepore Track-Etch Membrane, 200 nm pore size; Whatman plc, UK). After sizing, the liposomes were filter-sterilized using a 0.45-μm syringe filter (Asahi Techno Glass Co., Chiba, Japan).

The liposome concentration was determined using a phosphorus assay. BLs were prepared from liposomes and perfluoropropane gas (Takachiho Chemical Inc. Co. Ltd., Tokyo, Japan). First, 5-mL sterilized vials containing 2 mL of liposome suspension (lipid concentration: 1 mg/mL) were filled with perfluoropropane gas, capped, and then pressurized with 7.5 mL of perfluoropropane gas. The vials were placed in a bath sonicator (42 kHz, 100 W, Bransonic 2510J-DTH; Branson Ultrasonics Co., Danbury, CT) for 5 min to form BLs. The zeta potential and mean size of the BLs were determined using a light scattering method with a zeta potential/particle sizer, (Nicomp 380ZLS, Santa Barbara, CA). For preparation of BLs containing 1,2-dioleoyl-3-trimethylammonium-propane (DOTAP), we used phosphate-buffered saline (PBS) and 1,2-distearoyl-sn-glycero-3-phosphoethanolamine-N-[methoxy(polyethylene glycol)-750] (PEG_{750}) and DPPC, DOTAP, PEG_{2000}, and PEG_{750} were mixed at a molar ratio of 79:15:2:4, as described previously [21].

2.2. Ultrasound imaging

Male ICR mice were anesthetized, and injected with a BL solution in HBS into the tail vein. Examination of the heart or the ischemic hindlimb was performed using an Aplio80 ultrasound diagnostic machine (Toshiba Medical Systems, Tokyo, Japan) and a 12-MHz wideband transducer with contrast harmonic imaging at a mechanical index of 0.27. The mean intensity at various time points after injection into the ROI (region of interest) was quantified.

2.3. Cell lines and cultures

COS-7 cells were cultured in Dulbecco's modified Eagle's medium (DMEM; Kohjin Bio Co. Ltd., Tokyo, Japan), supplemented with 10% heat-inactivated fetal bovine serum (FBS; Equitech Bio Inc., Kerrville, TX), 100 units/mL penicillin, and 100 μg/mL streptomycin in a humidified atmosphere containing 5% CO_2 at 37 °C.

2.4. Plasmid DNA (pDNA)

The plasmid pcDNA3-Luc, derived from pGL3-basic (Promega, Madison, WI), is an expression vector encoding the firefly luciferase gene under the control of a cytomegalovirus promoter. The plasmid pBLAST-hbFGF (InvivoGen Inc., San Diego, CA) is an expression vector encoding the human bFGF gene controlled by an EF-1α promoter. The plasmid pBLAST is used as an empty vector control. Fluorescein-labeled pDNA (Label IT Plasmid Delivery Control) was purchased from Mirus (Madison, WI).

2.5. Preparation of p-BLs

For the preparation of p-BLs, adequate amounts of pDNA were added to BLs and gently mixed. To quantify the amount of pDNA loaded onto the BL surfaces, the BLs were centrifuged at 2000 rpm for 1 min, and the unbound pDNA was removed as previously reported [23]. The BL solution and aqueous solution containing unbound pDNA were then boiled for 5 min to solubilize the BLs and prevent background scattering. The optical density was measured at 260 nm using a spectrophotometer.

2.6. Stability of pDNA in the presence of serum

pDNA and p-BLs were incubated in 50% fetal bovine serum for 15–60 min. Serum was used without heat inactivation. To remove lipids and serum proteins, pDNA was extracted using a GenElute Mammalian Genome DNA Miniprep kit (Sigma–Aldrich, St. Louis, MO, USA). pDNA stability was confirmed via 1% agarose gel electrophoresis. The gel was stained with SYBR SAFE (Invitrogen Japan K.K., Tokyo, Japan) DNA stain and visualized under ultraviolet light.

2.7. Transfection of pDNA into cells using p-BLs and US

The day before transfection, 3×10^4 cells were seeded in the wells of a 48-well plate (Asahi Techno Glass Co., Chiba, Japan). p-BLs (BLs 60 μg, pcDNA3-Luc 5 μg) in culture medium containing 10% FBS were added to the cells. The cells were immediately exposed to US (Frequency, 2 MHz; duty, 50%; burst rate, 2.0 Hz; intensity 2.0 W/cm^2) for 10 s through a 6-mm diameter probe placed in the well. A Sonopore 3000 (NEPA GENE, Co., Ltd., Chiba, Japan) was used to generate the US. The cells were washed twice with culture medium and cultured for two days. To measure luciferase activity after transfection, cell lysate was prepared using a lysis buffer (0.1 M Tris–HCl (pH 7.8), 0.1% Triton X-100, and 2 mM EDTA). Luciferase activity was measured using a luciferase assay system (Promega, Madison, WI) and a luminometer (LB96V, Belthold Japan Co., Ltd., Tokyo, Japan). The activity is reported as relative light units (RLU) per mg of protein.

2.8. Hemolysis assay

Erythrocytes from mice were washed three times at 4 °C by centrifugation at 1000 rpm (Kubota 3700, Kubota, Tokyo, Japan) for 10 min and resuspended in PBS. A 5% stock suspension was prepared. Various BLs were added to the erythrocytes (BLs:stock suspension = 1:1) and incubated for 4 h at 37 °C. After incubation, the suspensions were centrifuged at 1000 rpm for 5 min, and supernatants were taken. Hemolysis was quantified by measuring the absorbance of hemoglobin at a wavelength of 540 nm. Lysis buffer was added to erythrocytes and used for the 100% hemolysis sample.

2.9. Hindlimb ischemia model

The ischemic hindlimb model was performed in five-week-old male ICR mice, as previously reported [24,25]. Briefly, animals were anesthetized, and a skin incision was made in the left hindlimb. After ligation of the proximal end of the femoral artery at the level of the inguinal ligament, the distal portion and all side branches were dissected and excised. The right hindlimb was kept intact to control the original blood flow. Measurements of the ischemic (left)/normal (right) limb blood flow ratio were performed for a set time using a laser Doppler blood flow meter (OMEGAFLO, FLO-C1).

2.10. In vivo luciferase gene delivery into the skeletal muscle of mice using BLs and US

Ten days after ligation of the femoral artery, a solution of 225 μL of p-BLs (BLs 200 μg, pcDNA3-Luc 50 μg) was injected into the tail vein, and the site of the hindlimb ischemia was immediately exposed to US (Frequency: 1 MHz, Duty: 50%, Burst rate: 2.0 Hz, Intensity: 1.0 W/cm^2, Time: 2 min). A Sonitron 2000 (NEPA GENE, Co., Ltd) was used as an ultrasound generator. Two days after transfection, the mice were euthanized. The thigh muscle in the US-exposed area was collected and homogenized in the lysis buffer. Luciferase activity was measured as described above.

2.11. The therapeutic effects of bFGF gene delivery with BLs and US

Ten and twelve days after ligation of the femoral artery, a solution of 225 μL of p-BLs (BLs 200 μg, pBLAST-hbFGF or pBLAST 50 μg) was injected into the tail vein, and US exposure (Frequency: 1 MHz, Duty: 50%, Burst rate: 2.0 Hz, Intensity: 1.0 W/cm^2, Time: 2 min) was immediately applied at the site of hindlimb ischemia. A Sonitron 2000 (NEPA GENE, Co., Ltd) was used as an ultrasound generator. Blood flow was measured several days after the second injection.

Four days after the second injection, the mice were euthanized, and the thigh muscle in the US-exposed area was collected. Total RNA was extracted with RNAiso Plus (Takara Bio Inc., Japan) according to the manufacturer's instructions. Complementary DNA was synthesized from 1 μg total RNA in a 20 μL reaction using Prime Script Reverse Transcriptase (Takara Bio Inc., Japan). Real-time RT-PCR was performed using an ABI PRISM 7000 Sequence Detection System instrument and software (Applied Biosystems Inc., Foster City, CA) with SYBR GreenER from Invitrogen. The primer sequences were previously described [21]. The amplification of the 18S ribosomal RNA gene was used as a control for RNA integrity and for assay normalization.

2.12. In vivo studies

Animal use and relevant experimental procedures were approved by the Tokyo University of Pharmacy and Life Sciences Committee on the Care and Use of Laboratory Animals. All experimental protocols for animal studies were in accordance with the Principle of Laboratory Animal Care in Tokyo University of Pharmacy and Life Sciences.

2.13. Statistical analyses

All data are represented as the mean ± SD (n = 3–6). Data were considered significant when $P < 0.05$. A t-test or one-way ANOVA was used to calculate statistical significance.

3. Results

We initially investigated the efficacy of BLs containing cationic lipids as US contrast agents. We performed US imaging of the heart after injecting of BLs via the tail vein and assessed the intensity of imaging effects. As shown in Fig. 1, all three types of BLs could be used as US contrast agents and are more stable than the BLs containing DOTAP that were previously reported [21,22]. BLs containing DSDAP were most effective of the three cationic lipids.

We examined the interaction of pDNA with each BL. As shown in Fig. 2, 30–40% of pDNA was loaded by BLs. The size of all BL types was 600–700 nm, and their zeta potential was almost neutral. Furthermore, adding pDNA to BLs did not result in a significant change in those physical properties (Table 1). We also investigated the stability of pDNA in 50% serum. Fig. 3 shows an image of free pDNA and p-BLs in the presence of serum for 15–60 min. The high-mobility band in the non-incubated samples was attributed to the most compact (supercoiled) form, whereas the other bands were considered to contain the non-supercoiled content in the plasmid preparation. The loss of the supercoil increased with longer incubation times; however, pDNA loaded onto BLs containing cationic lipid was more stable than free pDNA. Previously, we showed that p-BLs containing DOTAP could protect pDNA from serum components [21]. The result, however, showed a loss of the supercoiled conformation after incubation for 60 min, whereas the protective effects of the three types of BLs shown in this study could be observed even after incubation for 60 min.

To evaluate the ability of the BLs to induce cavitation which has been proposed as a driving force for gene transfection, we transfected pDNA into cells *in vitro*. Our results show that all BL types can be used for transfection and that BLs containing DSDAP were the most effective of the three cationic lipids (Fig. 4). We further investigated the cytotoxicity of type of BL. Cytotoxicity was absent after the transfection with p-BLs and US (data not shown). It has been reported that cationic liposomes often cause the agglutination

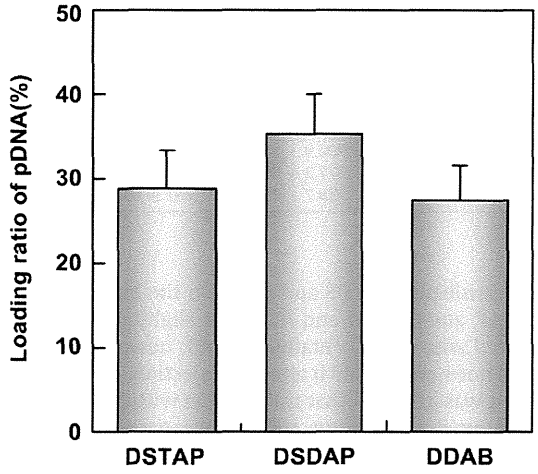

Fig. 2. Loading ratio of pDNA onto BLs. The ratio was calculated by measuring the optical density of a solution of p-BLs containing pDNA (15 μg) and various BLs (60 μg) after the removal of unbound pDNA via centrifugation.

of erythrocytes and high levels of hemolysis due to the interaction of the lipid component with the erythrocyte membrane [26,27]. Therefore, we also assessed the interaction of each BL with erythrocytes using an agglutination test and a hemolysis assay *in vitro*. No agglutination was observed in any BL type (data not shown). Furthermore, all BLs showed negligible hemolysis after a 4-hr incubation (Fig. 5). These results suggest that BLs containing cationic lipids have little effect on erythrocytes.

To evaluate the usability of p-BLs as a pDNA delivery tool via intravascular injection, we used the hindlimb ischemia mouse model. Before *in vivo* transfection using p-BLs and US, we first confirmed whether each p-BL was accessible to the ischemic hindlimb using US diagnostic equipment. The delivery of each p-BL to the ischemic hindlimb was observed and the signal intensity from p-BLs containing DSDAP had largest increase (Fig. 6a, b). We then transfected pDNA encoding the luciferase gene into the ischemic hindlimb. As shown in Fig. 6c, the combination of US and p-BLs containing DSDAP was the most effective. We also examined the

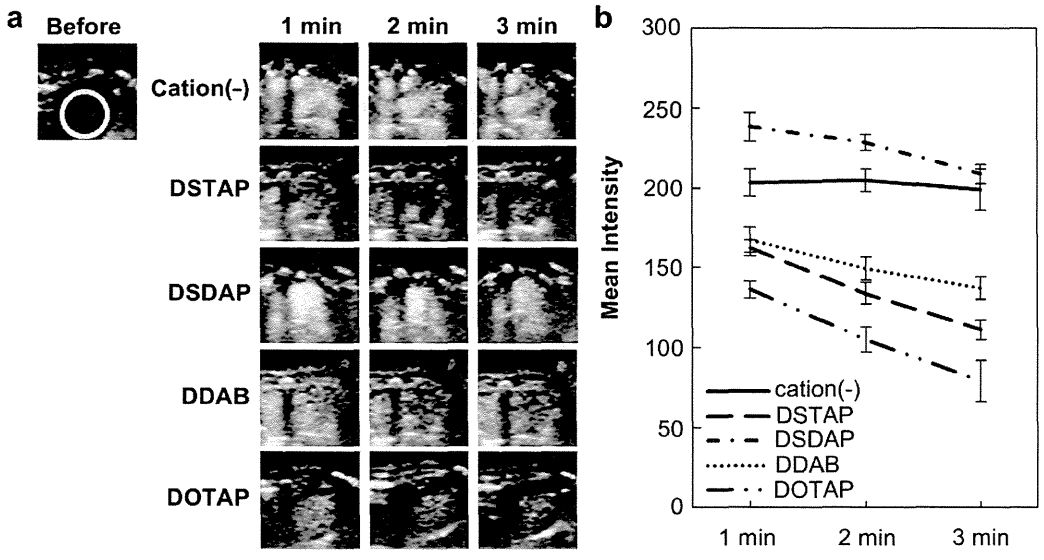

Fig. 1. (a) Ultrasonographic images of the heart using various BLs (1 mg/mL, 30 μL) containing cationic lipids 1–3 min after injection. Yellow circles show the region of interest (ROI). (b) Mean intensity of the pixels within the ROI. (For interpretation of the references to color in this figure legend, the reader is referred to the web version of this article.)

Table 1
Size and zeta potential of BLs or p-BLs.

	Mean size (nm)		Zeta potential (mV)	
	BLs	p-BLs	BLs	p-BLs
Cation(−)	636.5 ± 84.0	655.6 ± 72.2	0.22 ± 0.01	−0.39 ± 0.11
DSTAP	742.0 ± 85.6	906.9 ± 82.7	−0.36 ± 0.14	−1.81 ± 0.40
DSDAP	623.7 ± 82.8	577.2 ± 52.8	−0.17 ± 0.37	−2.66 ± 0.07
DDAB	700.8 ± 84.7	738.7 ± 97.5	−0.61 ± 0.85	−1.94 ± 0.89

effects of transfection via US and p-BLs on the biochemical values AST, ALT, ALP, and CK. AST and ALT were slightly increased in the group treated with p-BLs containing DDAB; however, those values returned to normal levels 48 h after the injection (data not shown). Therefore, it was assumed that transfection with p-BLs and US had little effect on liver function and muscle tissues. These results suggest that p-BLs containing DSDAP were the most effective as a US contrast agent and pDNA delivery tool compared to other BLs.

To determine the efficacy of the therapeutic effect, we transfected pDNA encoding bFGF into the ischemic hindlimb using US and p-BLs contained DSDAP. As a result, the mRNA levels of various angiogenic factors significantly increased, and the blood flow rate in the group treated with the bFGF gene also significantly improved compared to the control group, which was treated with saline or empty vector (Fig. 7). These results suggest that the combination of p-BLs containing DSDAP and US exposure could be a useful tool as a systemic gene delivery system and could be applicable to hindlimb ischemia therapy.

4. Discussion

Recently, the integration of diagnostic imaging capability with therapy is expected for clinical use, and theranostic agents have received a great deal of research interest [3]. US imaging is one of the most widespread diagnostic modalities used in clinics. Moreover, a combination of microbubbles and US has been proposed as a less invasive and tissue-specific intracellular delivery for molecules such as dextran, pDNA, peptides, and siRNA both *in vitro* and *in vivo* [10–15,28,29]. However, the accessibility of microbubbles is restricted because of their size.

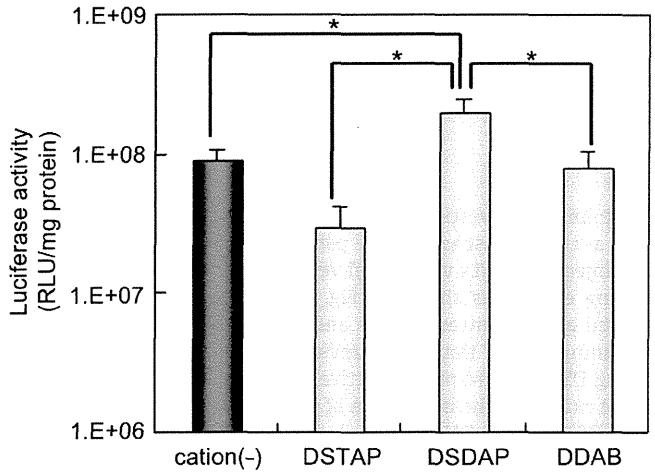

Fig. 4. Luciferase expression by cells transfected with pDNA using p-BLs and US. Luciferase expression in COS-7 cells transfected with pDNA (5 μg) using p-BLs (60 μg) and ultrasound (Frequency: 2 MHz, Duty: 50%, Burst rate: 2.0 Hz, Intensity: 2.0 W/cm^2, Time: 10 s) at 2 days post-transfection. All data represent the mean ± SD (n = 4).* indicates $P < 0.05$ using a one-way ANOVA with Tukey's post hoc test.

We previously developed nanosized pDNA-loaded BLs (p-BLs) and siRNA-loaded BLs (si-BLs) using DOTAP and demonstrated that the loading of nucleic acids onto BL improved the stability of the nucleic acids, and the effects of nucleic acids delivery were observed [21,22]. However, the gas retention ability of BLs containing DOTAP was lower than that of conventional BLs, and there remains room for improvement in their usability as a US contrast agent. It is known that short-chain and unsaturated fatty acids increase membrane fluidity [30]. DOTAP is unsaturated fatty acid and is thought to destabilize the membrane of BLs. In fact, the increased DOTAP content made it difficult to entrap the gas [22].

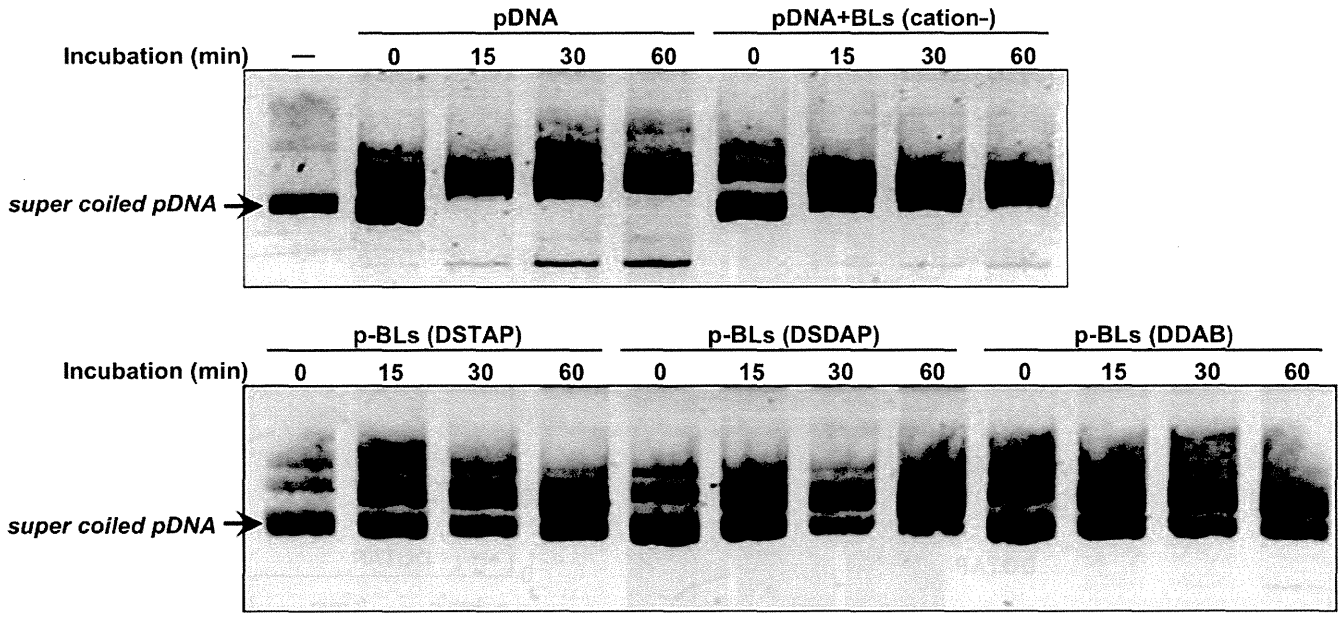

Fig. 3. Stability of pDNA in the presence of serum. Naked pDNA or p-BLs were subjected to 50% serum degradation at 37 °C for 15, 30, or 60 min and visualized via 1% agarose gel electrophoresis.

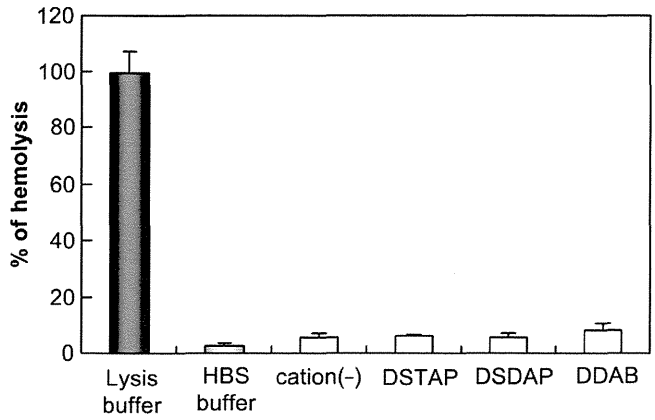

Fig. 5. Hemolysis test of BLs containing cationic lipids. Red blood cell suspensions were incubated with BLs or buffer for 4 h at 37 °C.

We therefore expected that p-BLs using other saturated cationic lipids would improve the stability of the liposomal membrane. Indeed, the three types of BLs tested here were more effective as a contrast agent compared to BLs containing DOTAP (Fig. 1). These results suggested that changing of the cationic lipid led to membrane stabilization and an improved gas retention ability.

The presence of nuclease in serum causes the degradation of DNA, which results in a loss of supercoiled content and leads to decreased transfection efficiency [31]. It has also been reported that the retention of the pDNA-supercoiled structure results in high transfection efficiency [32–34]. The proportion of pDNA loaded by BLs containing cationic lipid was 30–40%; however, loading onto the surface of BLs provided effective protection of pDNA against serum (Figs. 2 and 3). In contrast, free pDNA in solution or the mixture of pDNA and conventional BLs was not protected. Moreover, there were no significant changes in size and zeta potential after adding pDNA. These data suggested that pDNA was bound to the surface of BLs and that pDNA was protected by the fixed aqueous layer formed with PEG. Unexpectedly, there was no significant difference in the loading ratio and the pDNA protective effect among three types of BLs, although the acid dissociation constant (*pKa*) of DSDAP was low compared with that of DSTAP and DDAB. Furthermore, conventional BLs not containing cationic lipids also loaded small amounts of pDNA (data not shown). These results suggest that pDNA can be loaded not only by electrostatic interactions but also by the fixed aqueous layer formed with PEG. We also speculate that the stability of the membrane has some effect on the loading of pDNA. BLs with DSDAP might have a stable lipid membrane and could thus be useful both for US imaging and loading the pDNA.

The protective effects of the p-BLs tested here on pDNA were more pronounced than those of p-BLs containing DOTAP, although the pDNA loading ratios were roughly equivalent (data not shown). The difference in the protective effects might be due not only to the stability of membrane but also to the difference in cationic lipid content. BLs with DSTAP, DSDAP, or DDAB might be able to load pDNA more tightly than BLs with DOTAP. Therefore, the resistance to nuclease could improve. To maintain the integrity of pDNA in serum, pDNA should be stably held by BLs; however, US exposure should induce the cavitation of p-BLs, causing the pDNA to be released from the surface of BLs and transfected into cells. Prior to transfection experiments *in vivo*, we investigated the effect of gene delivery by p-BLs and US exposure *in vitro*. US exposure induced cavitation in all BLs and effective gene expression was observed (Fig. 4). Among them, the gene expression with p-BLs containing DSDAP was the highest. The difference in gene delivery effects

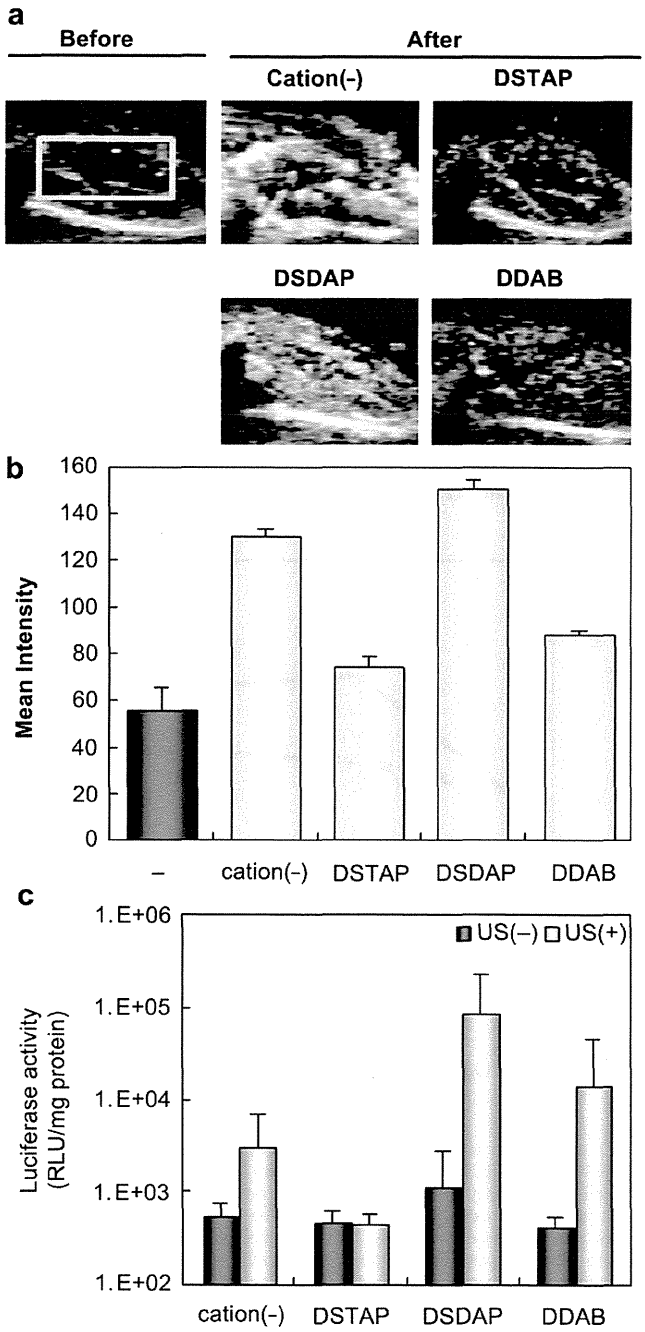

Fig. 6. (a) Ultrasonographic images of ischemic hindlimbs by various p-BLs (1 mg/mL, 200 μL) containing cationic lipids 30 s after injection. Yellow squares indicated the ROI. (b) Mean intensity of the pixels within the ROI. (c) Luciferase expression in ischemic muscle transfected with pDNA (50 μg) using p-BLs (1 mg/mL, 200 μL) and ultrasound (Frequency: 1 MHz, Duty: 50%, Burst rate: 2.0 Hz, Intensity: 1.0 W/cm^2, Time: 2 min) at 2 days post-transfection. (For interpretation of the references to color in this figure legend, the reader is referred to the web version of this article.)

might be due to the gas retention ability, the hardness of liposomal membrane, or the response to US. However, the stability of p-BLs *in vivo* could be important for reaching a target site via systemic injection.

We also examined whether p-BLs could be delivered to the ischemic hindlimb via microvessels using a US imaging system. The US echo signal was detected 5–10 s after the injection of p-BLs (Fig. 6a, b). The US imaging data for each BL demonstrated